Journal of Hydrology: Regional Studies 12 (2017) 253–272

Contents lists available at ScienceDirect

Journal of Hydrology: Regional Studies

journal homepage: www.elsevier.com/locate/ejrh

Combined statistical and spatially distributed hydrological model for evaluating future drought indices in Virginia

Hyunwoo Kang, Venkataramana Sridhar*

Biological Systems Engineering Department (MC0303), Virginia Tech, 155 Ag Quad Lane, Blacksburg, VA 24061, United States

ARTICLE INFO

Keywords:
Drought projection
Climate change
Drought indices
SWAT model

ABSTRACT

Study region: Virginia, United States.
Study focus: Climate change is expected to impact the intensity and severity of droughts; therefore, it is necessary to simulate future drought conditions using temperature and precipitation projections and hydrological models to derive reliable hydrological variables and drought indices. The objective of this study was to evaluate climate change influences on future drought potential and water resources in five major river basins in Virginia. In this study, the Soil and Water Assessment Tool (SWAT) and Coupled Model Intercomparison Project Phase 5 (CMIP5) climate models were used to compute a Standardized Soil Moisture Index (SSI), a Multivariate Standardized Drought Index (MSDI), and a Modified Palmer Drought Severity Index (MPDSI) for both historic and future periods. The drought conditions were evaluated, and their occurrences were determined at river basin scales.
New hydrological insights for the region: The results of the ensemble mean of SSI indicated that there was an overall increase in agricultural drought occurrences projected in the New (> 1.3 times) and Rappahannock (> 1.13 times) river basins due to increases in evapotranspiration and surface and groundwater flow. However, MSDI and MPDSI exhibited a decrease in projected future drought, despite increases in precipitation, which suggests that it is essential to use hybrid-modeling approaches and to interpret application-specific drought indices that consider both precipitation and temperature changes.

1. Introduction

Drought is one of the most prevalent natural hazards, adversely impacting water resources, the environment, agriculture, and the economy (Sternberg, 2011; Vasiliades and Loukas, 2009). Droughts have been occurring frequently in many parts of the world, and their impacts are being exacerbated by climate change (Dai, 2011). More specifically, global surface temperatures will continue to increase due increases in greenhouse gas emissions (IPCC, 2007; Qin et al., 2014; Pachauri et al., 2014). A warming climate will also lead to an increase in extreme climatic events, such as floods and droughts worldwide (Leonard et al., 2014). Evaluation of future drought incidence is fundamental to water resources management and planning, and this requires investigation of historical droughts and their impacts (Mishra and Singh, 2010 Sehgal et al., 2017).

In recent decades, the frequencies and severities of drought conditions in the United States have increased significantly (Changnon et al., 2000; Karl et al., 2012). Approximately 10% of the total U.S. experienced either severe or extreme droughts at one time during the 20th century (NCDC, 2002). Specifically, droughts can explain 17% of all weather-related disasters that occurred in

* Corresponding author.
E-mail address: vsri@vt.edu (V. Sridhar).

http://dx.doi.org/10.1016/j.ejrh.2017.06.003
Received 20 January 2017; Received in revised form 24 May 2017; Accepted 6 June 2017

the U.S. between 1980 and 2003 (Ross and Lott, 2003). The western region is currently experiencing one of the most severe droughts the country has never seen, which started in 2012 (Diffenbaugh et al., 2015; Mao et al., 2015). This drought was exacerbated by low winter precipitation and reduced mountain snowpack (Mao et al., 2015), which are both linked to global warming (AghaKouchak et al., 2014; Swain et al., 2014). Furthermore, climate model projections, based on multiple global climate models (GCMs), suggest that drying trends in precipitation, streamflow, and soil moisture can occur over many areas in low- and mid-latitudes due to increasing greenhouse gas (GHG) concentrations (Dai, 2013; Rajsekhar et al., 2015; Kumar et al., 2014; Chen and Sun, 2015; Mishra et al., 2014; Dai, 2011; Wang, 2005; Burke et al., 2006; Sheffield et al., 2012). More specifically, there is a strong tendency for wet areas to get wetter and dry areas to get drier, with a poleward expansion of the subtropical dry zones (Tallaksen and Van Lanen, 2004).

To identify and understand specific characteristics of regional drought, spatio-temporal observations of hydrological variables, such as runoff, soil moisture, and evapotranspiration (ET), are needed (Mo, 2008). Furthermore, satellite remote-sensing data can also provide essential information for identifying drought conditions with high spatio-temporal resolution (Wang et al., 2016). Specifically, they can provide insights into how human activities and land processes respond to drought conditions (Mu et al., 2012; Svoboda et al., 2002). However, since long-term and fine-resolution observations are sparse, large-scale hydrological models are used to simulate the land surface water and energy fluxes as well as hydrological variables, such as soil moisture, ET, and runoff, which are subsequently used to assess historic and future drought characteristics under climate change scenarios (Lakshmi et al., 2004; Mishra et al., 2010; Wang et al., 2011). For example, the Soil and Water Assessment Tool (SWAT) (Arnold et al., 1998) is an effective method to simulate and quantify the impact of climate change on the hydrological cycle and on drought conditions (Wu and Johnston, 2007; Jha et al., 2004). Furthermore, SWAT has been successfully applied to simulate water quantity over a wide range of scales and environmental conditions (Schuol et al., 2008) and to evaluate various types of drought, including meteorological, agricultural, and hydrological drought (Wang et al., 2011). It is possible that hydrological models can be the basis for evaluating drought conditions through the development of multiple drought indices, mitigation, and management strategies (Narasimhan and Srinivasan, 2005).

In recent decades, several drought indices have been developed to quantify meteorological, agricultural, and hydrological droughts. Generally, drought indices are computed to define drought and the related parameters, such as intensity, duration, and severity (Mishra and Singh, 2010). Drought indices are useful for drought detection (Niemeyer, 2008), assessing the onset and recovery (Tsakiris et al., 2007), declaring drought levels (intensity or severity), evaluating droughts (Niemeyer, 2008), drought forecasting, and future drought projection. For instance, the Standardized Precipitation Index (SPI) was proposed and used as a meteorological drought-monitoring tool (McKee et al., 1993). It is one of the most popular indices for quantifying meteorological drought (Zargar et al., 2011; Mishra and Singh, 2009). SPI is based on long-term precipitation records by transforming the cumulative probability of precipitation over a specific time period. These data are fit to a particular probability distribution (e.g., Gamma distribution), which is then transformed into a normal distribution with an SPI mean value of zero (McKee et al., 1993; Edwards, 1997). The framework of SPI computation serves as the basis for Standardized Soil Moisture Index (SSI; Hao and AghaKouchak, 2013) applied to monitor agricultural drought, which uses soil moisture as an input. Furthermore, SPI finds its application in quantifying future drought projections (Loukas et al., 2008; Liu et al., 2013). Generally, the mean value of the precipitation total is set to zero, values above zero indicate wet conditions, and values below zero indicate dry conditions (Table 1). Another popular drought metric is the Palmer Drought Severity Index (PDSI; Palmer, 1965); however, several shortcomings of PDSI have been documented (Alley, 1984), which have led to alternative indices.

Despite all of these efforts, one of the key problems that exist today in identifying droughts is the need for a single hydrological or meteorological indicator, which is lacking due to the inherent difficulty in obtaining many variables over large areas. This compromises the development of reliable risk assessment and drought management plans (Hao and AghaKouchak, 2013). To address these limitations, a Multivariate Standardized Drought Index (MSDI), based on multiple hydroclimatic variables, was developed and applied to quantify past droughts in the United States (Hao and AghaKouchak, 2013, 2014).

By employing large-scale hydrological models and multiple drought indices, numerous studies have investigated future droughts and the impacts of climate change on droughts in the southwestern and central United States (Hoerling and Eischeid, 2007; Gutzler and Robbins, 2011; Seager et al., 2007; Strzepek et al., 2010). Even though severe and significant droughts have affected the southeastern U.S. in recent decades (Wilhite and Hayes, 1998; Changnon et al., 2000; VDEM, 2013), there are few studies available that provide future drought projections based on high-resolution and physically based hydrological models, multiple drought indices, and climate change projections for this region. For instance, several regions in Virginia have experienced extreme drought as recent as 2007 or 2012, but these droughts were not fully understood due to the lack of comprehensive data and the difficulty in evaluating

Table 1
Classification of SPI, SSI, and MSDI values (McKee et al., 1993).

SPI values	Drought category
2.0 and above	Extremely wet
1.5 to 1.99	Very wet
1.0 to 1.49	Moderately wet
−0.99 to 0.99	Near normal
−1.0 to −1.49	Moderate drought
−1.50 to −1.99	Severe drought
−2.0 or more	Extreme drought

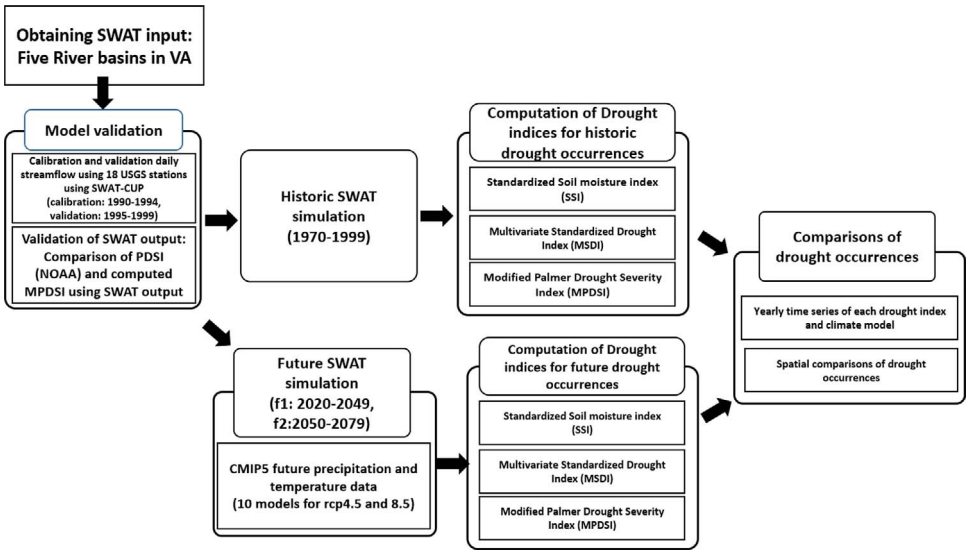

Fig. 1. Flow diagram of the overall processes of hydrological modeling and drought projection.

the rate of incidence (VDEM, 2013). It is imperative that the evaluation of future drought conditions employs a reliable hydrological model, dependable drought indices, and high-resolution climate change projections to effectively characterize drought.

Thus, the objective of this study was to evaluate the impacts of climate change on the occurrence of droughts in five major river basins in Virginia, namely, the James, Roanoke, New, Rappahannock, and York river basins. This was achieved by using high-resolution datasets, a physically based hydrological model, and multiple drought indices to characterize the spatio-temporal changes of future droughts. To carry out these objectives, the SWAT model was applied to compute multiple drought indices for historic and future periods, with meteorological inputs from the Climate Modeling Intercomparison Project 5 (CMIP5) models. Based on physical interpretation of the simulated hydrological variables, which were used in computing the drought indices, the relative changes in both historic and future droughts were assessed. The following sections describe approaches, the results and discussion concerning projecting future conditions, which can provide better perspectives on the spatial heterogeneity of drought conditions across the study area.

2. Data and methods

Fig. 1 is a flow diagram of the overall approach and methods used in this study. First, input data required for SWAT for the five river basins were generated. Second, the model simulation was carried out at daily time steps using the observed streamflow with both calibration and validation from multiple gaging stations, and the simulations were verified for the accuracy of the model estimates. After gaining confidence in the streamflow estimates, it was assumed that other water budget variables, including soil moisture and evapotranspiration, were suitable for computing the drought indices. Subsequently, three drought indices were computed and evaluated for both historical and future periods, and future drought conditions were evaluated using weekly time series, seasonal comparisons, and their spatial occurrences.

2.1. Study area

Our study area consisted of the James, Roanoke, New, Rappahannock, and York river basins in Virginia. These basins were selected because they cover 62% of the Commonwealth of Virginia and reflect hydrological and political boundaries that reflect the overall hydrological conditions in Virginia. Furthermore, these basins have experienced several severe droughts recently. The James, Rappahannock, and York river basins are the sub-basins of the Chesapeake Bay watershed, and the New River is part of the Ohio River basin. The total drainage area of the five river basins is 74,298 km^2 (James: 26,773 km^2, Roanoke: 24,117 km^2, New: 10,016 km^2, Rappahannock: 6544 km^2, and York: 6848 km^2). Fig. 2(a) shows the location and topography of the five river basins, and the location of stream gauge stations. Land-surface elevations range from 5 m at the eastern coastline to the western mountainous areas (1738 m). The mean annual precipitation for the James, Roanoke, New, Rappahannock, and York river basins are 1118 mm to 1172 mm. Furthermore, the mean annual temperature for the five river basins range from 13.15 °C to 13.90 °C. In addition, about sixty percent of the five basins consist of forest (58.85%), whereas the other forty percent is covered by pasture/hay (16.59%), developed areas (8.52%), cultivated crops (3.29%), and woody wetlands (3.85%).

Fig. 3(a) provides a time series of the mean values of PDSI from the National Oceanic and Atmospheric Administration (NOAA) (ftp://ftp.ncdc.noaa.gov/) and monthly precipitation data from 1970 to 2015 in Virginia; Fig. 3(b) represents the time series of PDSI values for each climate division. In the early and mid-1980s, late 1990s, and early and late 2000s, severe and extreme droughts struck these regions (event 1 and 2). Furthermore, there was severe drought in division 6 in the late 1980′s.

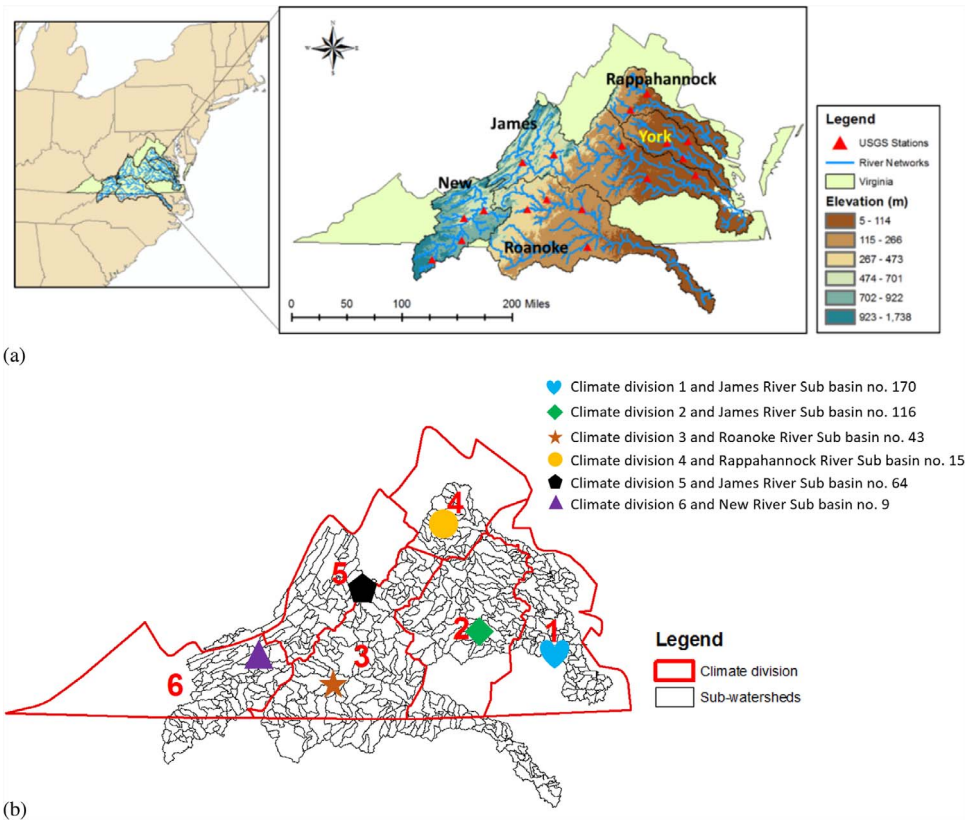

Fig. 2. Location map of the five river basins and climate divisions in Virginia. (a) Red triangles indicate USGS stream gauge stations, and blue lines represent the river networks. (b) Red lines indicate the climate divisions in Virginia, and black lines represent the sub-watersheds in the five river basins.

2.2. Hydrological simulation model

The Soil and Water Assessment Tool (Arnold et al., 1998) is a physically based hydrological model that simulates large river basins continuously. SWAT has been widely used in research to simulate hydrology and water quality, as well as climate change

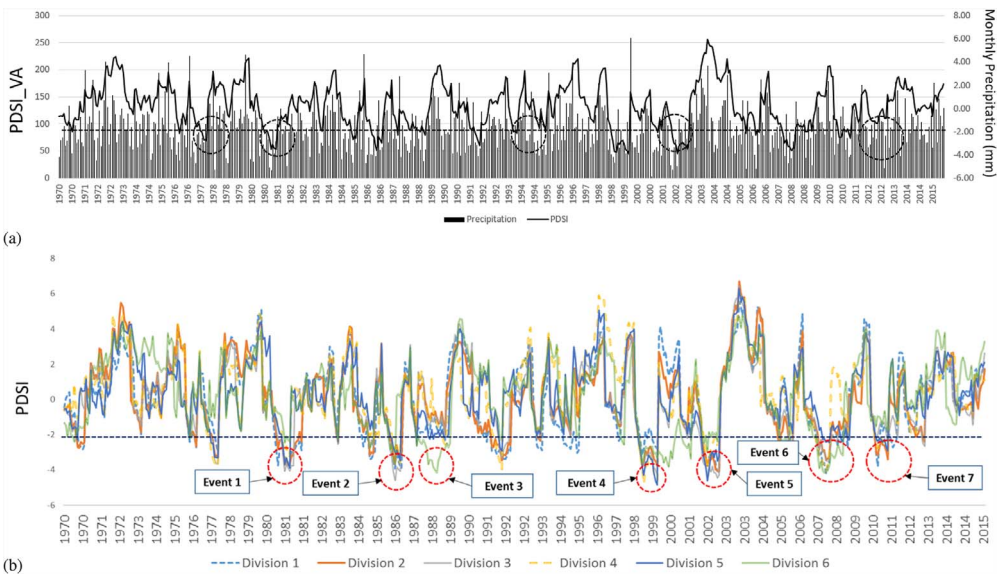

Fig. 3. Comparisons of (a) monthly precipitation and (b) PDSI in Virginia. The dashed horizontal line represents a moderate to extreme drought condition (-2 or less), and the red and dashed circles outline the drought events.

impacts on drought (Wang et al., 2011; Ahn et al., 2015; Ashraf Vaghefi et al., 2014). SWAT is based on the concept of hydrological response units (HRUs), which are a unique combination of soil, land cover, and slope. The hydrological cycle simulated by the SWAT model is based on a water balance equation (Eq. (1)).

$$SW_t = SW_0 + \sum_{i=1}^{t} P_{day} - Q_{surf} - E_a - W_{seep} - Q_{gw} \quad (1)$$

where, SW_t is the final soil water content (mm), SW_0 is the initial soil water content on day i (mm), t is the time (days), P_{day} is the amount of precipitation on day i (mm), Q_{surf} is the amount of surface runoff on day i (mm), E_a is the amount of evapotranspiration on day i (mm), W_{seep} is the amount of water entering the vadose zone from the soil profile on day i (mm), and Q_{gw} is the amount of return flow on day i (mm). SW_t was used to compute the Standardized Soil Moisture Index (SSI), Multivariate Standardized Drought Index (MSDI), and Modified Palmer Drought Severity Index (MPDSI), which were the drought indices used in this study. Additionally, E_a, Q_{surf}, and Q_{gw} were used to compute the MPDSI.

Furthermore, within the model, three storage volumes were represented for HRU, i.e., the unsaturated soil profile (0–2 m), the shallow aquifer (2–20 m), and the deep aquifer (> 20 m). Soil water and hydrological processes contained surface runoff, lateral flow, percolation to shallow and deep aquifers baseflow, infiltration, evaporation, and plant water uptake. The simulation of surface runoff was based on the modified SCS curve number (CN) method (USDA Soil Conservation Service, 1972) using daily precipitation data. For the estimation of evapotranspiration (ET) and potential ET (PET), the Penman-Monteith (Monteith, 1965) method was used in this study. ET and PET were also the input variables used to calculate MPDSI. The SWAT model required a digital elevation model (DEM), land use, soil, and daily values of meteorological data. In this study, a 100 m × 100 m DEM was used from the National Elevation Dataset (NED) (Gesch, 2007), land use was obtained from the National Land Cover Data (NLCD) (Homer et al., 2004), and a soil map was developed from State Soil Geographic data (STATSGO) (USDA, 1991) at a scale of 1:250,000.

Daily streamflow simulated by SWAT was calibrated and validated using the SWAT calibration and uncertainty assessment tool (SWAT-CUP) (Abbaspour, 2011). We identified eleven parameters and used them in a calibration and validation process (calibration: 1990–1994, validation: 1995–1999) (Table 2). Using the daily streamflow data from eighteen United States Geological Survey (USGS) stream gauge stations (Table 3, Fig. 2(a)) for calibration and validation, the model evaluation was carried out based on the Nash-Sutcliffe coefficient (NSE) (Nash and Sutcliffe, 1970) (Eq. (2)).

$$\mathrm{NSE} = \left(\frac{\sum_{i=1}^{n} Q_s - Q_{obs}}{\sum_{i=1}^{n} Q_{obs} - \overline{Q_o}} \right) \quad (2)$$

where Q_s is the simulated river discharge at time i, Q_{obs} is the observed river discharge at time i, and $\overline{Q_o}$ is the mean value of the observed flow in the calibration processes. NSE ranges from 1 (perfect match) to $-\infty$ and shows how well the plots of the observed and the estimated values fit with the 1:1 line.

2.3. Drought indices

In this study, SWAT was used to compute the input variables for multiple drought indices, such as the Standardized Soil Moisture Index (SSI), Multivariate Standardized Drought Index (MSDI), and Modified Palmer Drought Severity Index (MPDSI) (Mo and Chelliah, 2006) for evaluation of future droughts with CMIP5 climate models. For instance, SWAT-estimated SW_t was used for computing SSI, MSDI, and MPDSI. Furthermore, simulated ET, PET, and runoff were also used to calculate the MPDSI.

Several studies have investigated multivariate drought indicators using joint distribution and probability (Hao and Aghakouchak, 2013 AghaKouchak, 2015). Typically, joint probability provides the joint behavior of two random variables (X and Y). By adopting this approach, a Multivariate Standardized Drought Index (MSDI) was developed and applied using the joint probability of accumulated precipitation and soil moisture (Hao and Aghakouchak, 2013; AghaKouchak, 2015). The joint distribution of two variables

Table 2
Description of the SWAT input parameters selected for the streamflow calibration.

Parameter	Description	Min	Max
r_CN2.mgt	Curve number for moisture condition II	−0.2	0.2
v_ALPHA_BF.gw	Base flow alpha factor	0	1
v_GW_DELAY.gw	Ground water delay time	0	450
v_GWQMN.gw	Threshold water Depth in shallow aquifer for back discharge	0	2000
v_EPCO.hru	Plant uptake compensation factor	0.01	1
v_ESCO.hru	Soil evaporation compensation factor	0.01	1
v_SLSUBBSN.hru	Average slop length	10	150
v_OV_N.hru	Manning's *n* value for overland flow	0	0.8
v_CH_N2.rte	Manning's *n* value for main channel	0	0.3
v_CH_K2.rte	Main channel conductivity	0	150
v_SURLAG.bsn	Surface runoff lag coefficient	1	24

v_: denotes the default parameter is replaced by a given value, and r _: means the existing parameter value is multiplied by (1+ a given value).

Table 3
Description of the USGS stream gauge stations.

USGS station	Station Name	Latitude	longitude	Location
USGS02034000	RIVANNA RIVER AT PALMYRA	37°51′28”	78°15′58”	James River
USGS02024000	MAURY RIVER NEAR BUENA VISTA	37°45′45”	79°23′30”	James River
USGS02018000	CRAIG CREEK AT PARR	37°39′57”	79°54′42”	James River
USGS02042500	CHICKAHOMINY RIVER NEAR PROVIDENCE FORGE	37°26′10”	77°03′40”	James River
USGS02040000	APPOMATTOX RIVER AT MATTOAX	37°25′17”	77°51′33”	James River
USGS01664000	RAPPAHANNOCK RIVER AT REMINGTON	38°31′50”	77°48′50”	Rappahannock River
USGS01666500	ROBINSON RIVER NEAR LOCUST DALE	38°19′30”	78°05′45”	Rappahannock River
USGS03170000	LITTLE RIVER AT GRAYSONTOWN	37°02′15”	80°33′25”	New River
USGS03167000	REED CREEK AT GRAHAMS FORGE	36°56′20”	80°53′15”	New River
USGS03165000	CHESTNUT CREEK AT GALAX	36°38′45”	80°55′10”	New River
USGS03161000	SOUTH FORK NEW RIVER NEAR JEFFERSON	36°23′36”	81°24′25”	New River
USGS02059500	GOOSE CREEK NEAR HUDDLESTON	37°10′23”	79°31′14”	Roanoke River
USGS02062500	ROANOKE (STAUNTON) RIVER AT BROOKNEAL	37°02′22.0”	78°56′44.6”	Roanoke River
USGS02056900	BLACKWATER RIVER NEAR ROCKY MOUNT	37°02′42”	79°50′40”	Roanoke River
USGS02077670	MAYO CR NR BETHEL HILL	36°32′27”	78°52′19”	Roanoke River
USGS01674500	MATTAPONI RIVER NEAR BEULAHVILLE	37°53′02”	77°09′55”	York River
USGS01671100	LITTLE RIVER NEAR DOSWELL	37°52′21”	77°30′48”	York River
USGS01673550	TOTOPOTOMOY CREEK NEAR STUDLEY	37°39′45”	77°15′29”	York River

can be expressed as follows:

$$P(X \leq x, Y \leq y) = p \tag{3}$$

where p is joint probability of the precipitation and soil moisture. Furthermore, MSDI can be defined as follows (Hao and Aghakouchak, 2013):

$$\mathrm{MSDI} = \varnothing^{-1}(p) \tag{4}$$

where $\varnothing$ is the standard normal distribution function.

In the method described in Hao and AghaKouchak (2013), Eq. (4) was obtained using multivariate parametric copulas (Nelsen, 2006) and it required parameter estimation and goodness-of-fit tests. In this study, an alternative methodology to derive empirical joint probability, namely, Gringorten plotting position formulas, was used to alleviate the computational concern in fitting parametric distributions (Gringorten, 1963;Benestad and Haugen, 2007), and it can be described as follows:

$$P(x_k, y_k) = \frac{m_k - 0.44}{n + 0.12} \tag{5}$$

where m_k is the number of occurrences of the pair (x_i, y_i) for $x_i \leq x_k$ and $y_i \leq y_k$, and n is the number of the observation. After the joint probability was obtained from Eq. (5), it was used as an input to Eq. (4) to estimate the MSDI. To compute SPI and SSI, the univariate form of the Gringorten plotting position formula (Eq. (6)) (Gringorten, 1963) was also used:

$$P(x_i) = \frac{i - 0.44}{n + 0.12} \tag{6}$$

where n is the number of observations, and i is the rank of the measured values from the smallest. The rank of soil moisture value for historic (1970–1999), f1 (2020–2049), and f2 (2050–2079) period changes is integrated into our analysis. In other words, the time windows that we used allowed shifting means over time, suggesting that non-stationarity is included in the analysis. Since the GCM-based precipitation and temperature used in the simulation of soil moisture accounted for non-stationarity, when the relative change in SSI was calculated, it implicitly incorporated the changing conditions. Furthermore, to preserve the distinct changes on decadal scales, the analysis was split into 2 separate windows as the uncertainty in the GCM projections was expected to become larger later in the century.

Furthermore, the Modified Palmer Drought Severity index (MPDSI) (Mo and Chelliah, 2006) was also used to evaluate future drought conditions. There are shortcomings of PDSI, including the estimation of PET in the Thornthwaite (1948) formula, which is a method with surface temperature only and a parameterization of fixed available water capacity over the entire United States, which leads to the development of MPDSI. In this study, historic and future MPDSI values were computed using the input and output from SWAT and they were as follows: precipitation, ET, PET, soil moisture, and runoff. MPDSI uses water budget principles and the adjustment between the actual and climatological estimation known as “Climatically appropriate for existing conditions (CAFEC),” which is described as follows:

$$d = P - \mathrm{CAFEC}, \text{ where} \tag{7}$$

$$\mathrm{CAFEC} = \alpha\mathrm{PE} + \beta\mathrm{PR} + \gamma\mathrm{PRO} + \delta\mathrm{PL} \tag{8}$$

where PE is the potential evapotranspiration, PR is the potential recharge, PRO is the potential runoff, and PL is the potential soil

moisture loss; the coefficients α,β,γ,and δ are the ratio of the mean variables over the simulation period. More detailed descriptions of MPDSI are available from Mo and Chelliah (2006). In this study, the weekly time step of SSI, MSDI (25-week scale), and MPDSI were computed based on the input and output variables from the SWAT model, and they were used to evaluate future drought conditions in five river basins.

2.4. Climate models

The capability of a climate model to simulate present climate and historical tendencies leads to higher confidence in the projected future scenarios (Reifen and Toumi, 2009; Wuebbles et al., 2014). Numerous studies have reported increases in severity and frequency of droughts when extending the climate change model projections to determine hydrological outcomes (Sheffield and Wood, 2008; Dai, 2012). For example, CMIP5 provides multi-model simulations of historic and future climates, which are comparable to various greenhouse-gas (GHC) emissions scenarios (Taylor et al., 2012). Furthermore, the CMIP5 includes finer spatial resolution models, enhanced model physics, and an advanced set of output fields (Taylor et al., 2012). Additionally, the CMIP5 projections have a wider range of potential increases in global average temperatures, and the archive integrates advanced climate models with recent emission scenarios (Jin and Sridhar, 2012; Rogelj et al., 2012). Furthermore, CMIP5 with Bias-Correction Constructed Analogues (BCCA) and statistical downscaling used in this study (Brekke et al., 2013) addresses the aforementioned GCM biases and deficiencies; these approaches have been evaluated in hydrological impact studies (Taylor et al., 2012, Sridhar and Anderson, 2017; Jaksa and Sridhar, 2015). Several studies have evaluated the CMIP5 precipitation simulations at both global and regional scales (Feng et al., 2013; Sheffield et al., 2013; Hao et al., 2013; Schubert and Lim, 2013; Sillmann et al., 2013) and concluded that the multi-model ensemble mean of CMIP5 represents the observed spatial trends of hydroclimatic variables; these studies determined that future climate projections are robust. Specifically, Nasrollahi et al. (2015) investigated how well CMIP5 climate models explain historical wetting or drying trends, as well as their spatio-temporal patterns across the globe; their results indicate that most CMIP5 models agree with observed global trends in projecting the vulnerable areas for drought.

2.5. SWAT analysis for historic and future drought projections

The SWAT model was run at a daily time step for the historic (1970–1999) and projected future periods (f1: 2020–2049, f2:2050–2079) for each sub-basin with Representative Concentration Pathways (RCP) 4.5 and 8.5 scenarios (Table 4). There were 480 climate grid points in the five basins from the CMIP5 climate models at 1/8th degree resolution. Therefore, the delineation of watersheds in the five river basins was done in such a way as to consider all of the climate grids.

For the historic simulation, a calibration and validation of SWAT-estimated streamflow was carried out using daily streamflows from 18 USGS stations and the SWAT-CUP module to obtain an appropriate parameter set for each basin. Additionally, other SWAT outputs such as ET, PET, soil moisture, and runoff were implicitly validated with comparisons of PDSI from NOAA and with computed MPDSI from the SWAT output. Based on the results of the calibration and validation, both historic and future simulations were performed to compute drought indices (SSI, MSDI, and MPDSI). Additionally, a parameter uncertainty analysis of drought projections was performed using comparisons of the boxplot mean and 95% confidence intervals of each drought index for the five river basins (historic and future periods of each climate model). Finally, historic and future drought indices were compared based on weekly time series plots, as well as seasonal, and spatial analysis of drought occurrences.

Using the computed drought indices, historic and future drought occurrences were identified as a recognizable drought event when the SSI and MSDI values were less than −1 (moderate to extreme drought), and the MPDSI was less than −2 (moderate to extreme drought). Subsequently, to quantify the relative change in drought, the differences between the future and past drought occurrences were computed at a sub-basin level. The period of historic simulation was from 1970 to 1999, and future simulation was conducted during two time windows, 2020–2049 (f1), and 2050–2079 (f2).

Table 4
List of the CMIP5 General Circulation Model (GCMs) employed in this study.

Abbreviation	Name
S1	access1-0
S2	bcc-csm1-1.1
S3	canesm2
S4	ccsm4
S5	cesm1-bgc.1
S6	cnrm-cm5.1
S7	csiro-mk3-6-0
S8	gfdl-esm2g.1
S9	inmcm4
S10	ipsl-cm5a-mr

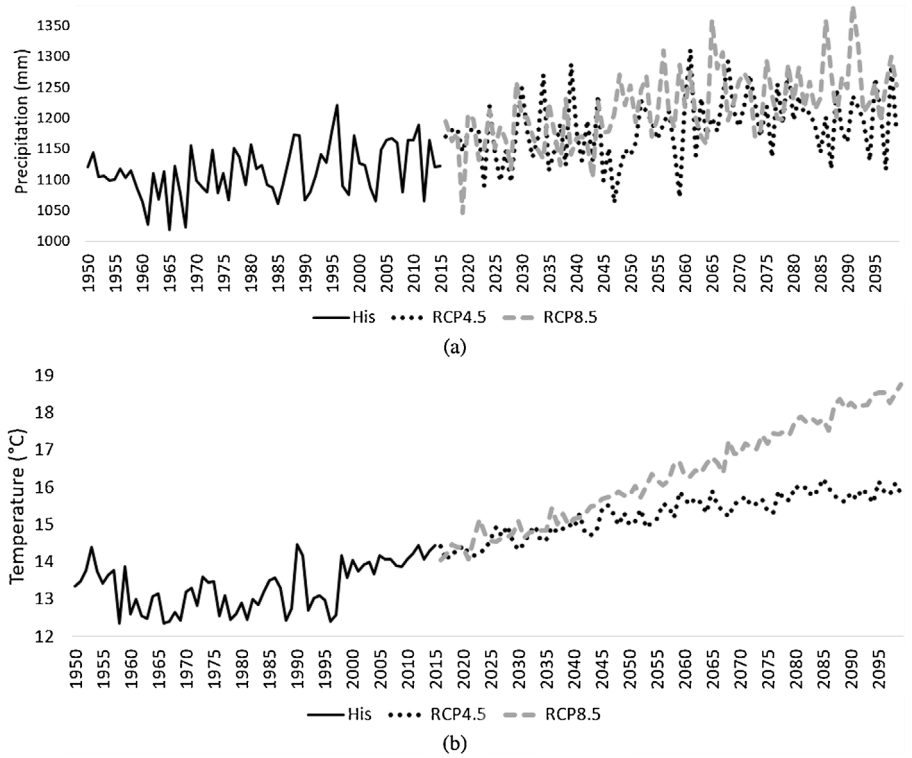

Fig. 4. (a) Annual precipitation and (b) temperature change. (a) The solid line represents the time series of annual precipitation during the historic period. The dashed lines represent the future period. (b) The solid line is the time series of the annual average temperature in the historic period. The dashed lines represent the future period.

3. Results and discussion

3.1. Past and future climate

Fig. 4 shows the time series of precipitation and temperature averaged over the five river basins. There were increasing precipitation and temperature trends for both ensemble means of RCP 4.5 and RCP 8.5. During the historic period (1970–1999), the mean annual precipitation was 1118 mm, and the mean annual temperature was 13.13 °C in the five river basins. Compared to the historic period, the results of RCP 4.5 indicate that the ensemble means of precipitation increased by 3.9% and 7.7%, and temperature increased by 1.65 °C and 2.34 °C in the f1 and f2 periods, respectively. Furthermore, the results of RCP 8.5 indicate that the ensemble mean precipitation increased by 5.6% and 10.5%, and the temperature increased by 1.92 °C, and 3.55 °C in the f1 and f2 periods, respectively.

Fig. 5 and Table 5 show the changes in precipitation and temperature for each CMIP5 model between the historic and future periods averaged over the five basins. The X-axis represents the change in precipitation (%), whereas the Y-axis represents the change in temperature (°C). The blue and green dots represent the precipitation and temperature change in the f1 period, and the red and yellow dots are for the f2 period. Generally, the magnitude of change in precipitation and temperature during the f2 period was higher than during the f1 period for both RCP 4.5 and RCP 8.5. More specifically, the maximum precipitation increase for RCP 4.5 was 17% in the S7 model during the f2 period, whereas there was a 3.4% decrease in precipitation in the S9 model during the f1 period. Furthermore, the maximum temperature increase for RCP 4.5 was 3.0 °C in the S1 model during the f2 period, whereas the minimum temperature increase was 0.9 °C in the S9 model during the f1 period. Furthermore, the maximum precipitation increase for RCP 8.5 was 20.7% in the S3 model during the f2 period, whereas there was a decrease in precipitation by 1.6% in the S9 model during the f2 period. Furthermore, the maximum temperature increase for RCP 8.5 was 4.3 °C in the S8 model during the f2 period, whereas there was an increase of 0.9 °C in temperature in the S9 model during the f1 period.

Fig. 6 shows the precipitation and temperature change for each CMIP5 model and river basin. In the case of the RCP 4.5 scenarios in the f1 period (Fig. 6(a)), the maximum precipitation increase was 7.71% in the S4 model for the New River basin, and the maximum temperature increase was 2.28 °C in the S3 model for the Rappahannock River basin. However, there was 7.12% decrease in precipitation in the S9 model for the Roanoke River basin, and the minimum temperature increase was 0.80 °C in the S9 model in the York River basin. For the RCP 4.5 and f2 period (Fig. 6(b)), the maximum precipitation increase was 15.83% in the S5 model for the York River basin, and the maximum temperature increase was 3.09 °C in the S3 model for the Rappahannock River basin. However, there was a 4.82% decrease in precipitation in the S2 model for the Roanoke River basin, and the minimum temperature increase was 1.11 °C in the S9 model for the York River basin.

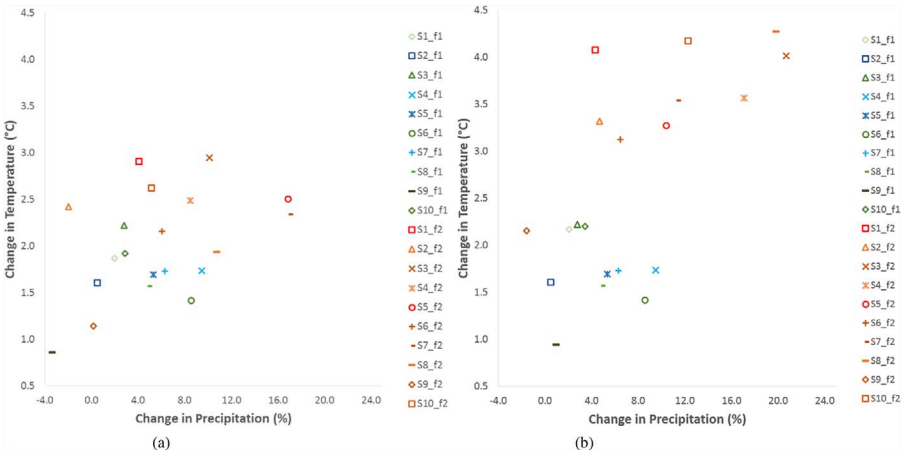

Fig. 5. Precipitation and temperature change in the five river basins: (a) RCP 4.5 and (b) RCP 8.5. The X-axis is the change in precipitation (%), and the Y-axis is the change in temperature (°C). All of the dots represent the change in precipitation and temperature for each climate model and time period. The blue and green dots represent the f1 period, whereas red and brown dots represent the f2 period.

For RCP 8.5 in the f1 period (Fig. 6(c)), the maximum precipitation increase was 10.77% from the S8 model in the New River basin, and the maximum temperature increase was 2.59 °C in the S3 model for the Rappahannock River basin. Additionally, there was a 3.38% decrease in precipitation in the S2 model in the Roanoke River basin, and the minimum temperature increase was 0.90 °C in the S9 model for the James River basin. Finally, in the case of RCP 8.5 in the f2 period (Fig. 6(d)), the maximum precipitation increase was 20.91% in the S3 model for the New River basin, and the maximum temperature increase was 4.44 °C in the S8 model in the Rappahannock River basin. In contrast, there was a 4.68% decrease in precipitation in the S9 model in the New River basin, and a minimum temperature increase of 2.09 °C in the S9 model for the James River basin.

Figs. 7 and 8 are the spatial maps of the ensemble mean for precipitation and temperature changes over all of the basins. As shown in Table 6, the increase in precipitation in the York River basin was highest. There were 2.25–5.92% increases in RCP 4.5, and 3.48–8.68% increases in RCP 8.5. However, the increase in precipitation in the Rappahannock River basin was lowest. There were 0.26–3.87% increases in RCP 4.5, and 1.85–7.12% increases in RCP 8.5. Furthermore, the temperature increase was highest in the Roanoke and Rappahannock River basins. Our calculations resulted in an increase in temperature between 1.71 (RCP4.5) to 1.96 °C (RCP8.5) in the Roanoke River basin during the f1 period, and an increase between 2.4 (RCP4.5) to 3.64 °C (RCP8.5) in the Rappahannock River basin during the f2 period.

3.2. Model evaluation and role of parameter uncertainty

In this study, the results of the simulation in the hydrology model that generated streamflow among other water budget components were calibrated and validated using SWAT-CUP, and the Sufi-2 process. The calibration period was from 1990 to 1994, and the validation period was 1995–1999. Table 7 shows the results of the calibration and validation for eighteen gaging stations, and for nearly all sites, the Nash and Sutcliffe Efficiency (NSE; Nash and Sutcliffe, 1970) values were larger than or close to 0.5, which was considered to be satisfactory for daily streamflow simulation (Moriasi et al., 2007). Furthermore, Fig. 9 shows the time series of the calibrated and validated streamflow at several locations.

Table 5
Changes in precipitation and temperature for each CMIP5 model.

CMIP5 model Abbreviation	RCP4.5				RCP8.5			
	Change in Precipitation (%)		Change in Temperature (°C)		Change in Precipitation (%)		Change in Temperature (°C)	
	f1	f2	f1	f2	f1	f2	f1	f2
S1	2.0	4.1	1.9	3.0	2.1	4.3	2.2	4.1
S2	0.5	−2.0	1.6	2.4	−0.3	4.7	1.9	3.3
S3	2.8	10.1	2.2	2.9	4.3	20.7	2.5	4.0
S4	9.5	8.5	1.7	2.5	10.9	17.1	1.8	3.6
S5	5.3	16.9	1.7	2.5	10.7	10.4	1.9	3.3
S6	8.6	6.1	1.4	2.2	3.2	6.4	1.7	3.1
S7	6.3	17.0	1.7	2.3	9.9	11.4	1.8	3.5
S8	4.9	10.7	1.6	1.9	11.3	19.8	2.2	4.3
S9	−3.4	0.2	0.9	1.1	0.9	−1.6	0.9	2.2
S10	2.9	5.1	1.9	2.6	3.4	12.3	2.2	4.2

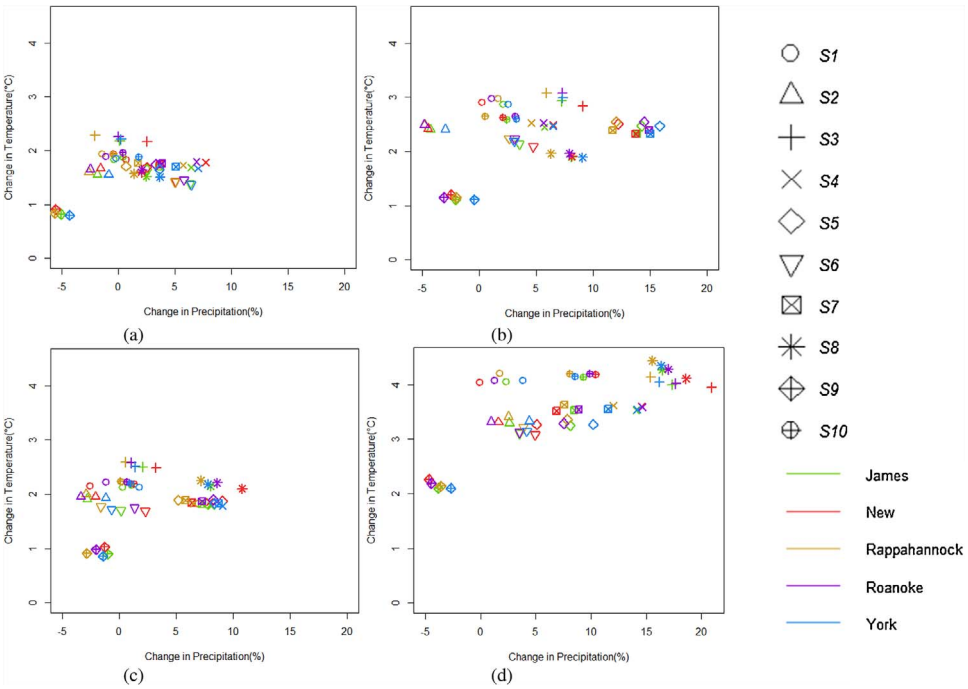

Fig. 6. Precipitation and temperature change in each river basin: (a) RCP 4.5 and f1 period (b) RCP4.5 and f2 period (c) RCP8.5 and f1 period and (d) RCP8.5 and f2 period. The different shapes of dots represent the change in precipitation and temperature in each river basin (green: James, red: New, brown: Rappahannock, purple: Roanoke, and blue: York).

Historical drought occurrences were also evaluated based on the comparisons of historic PDSI derived for each climate division from NOAA (ftp://ftp.ncdc.noaa.gov/) and the MPDSI values computed using the output variables from the SWAT simulation such as runoff, soil moisture, ET, and PET. Fig. 2(b) shows the climate divisions for Virginia and the locations of sub-watersheds that were used for comparisons of historic drought conditions. The PDSI values in climate division 1 were compared with MPDSI values from sub-watershed No. 170 in the James River basin, and climate division 2 was compared with sub-watershed No. 116 for the James River basin, climate division 3 was compared with sub-watershed No. 43 in the Roanoke River basin, climate division 4 was compared with sub-watershed No. 15 in the Rappahannock River basin, climate division 5 was compared with sub-watershed No. 64 in the James River basin, and climate division 6 was compared with sub-watershed No. 43 in the New River basin.

For each climate division and sub-watershed, historic drought events between 1970 and 1989 were evaluated to assess whether

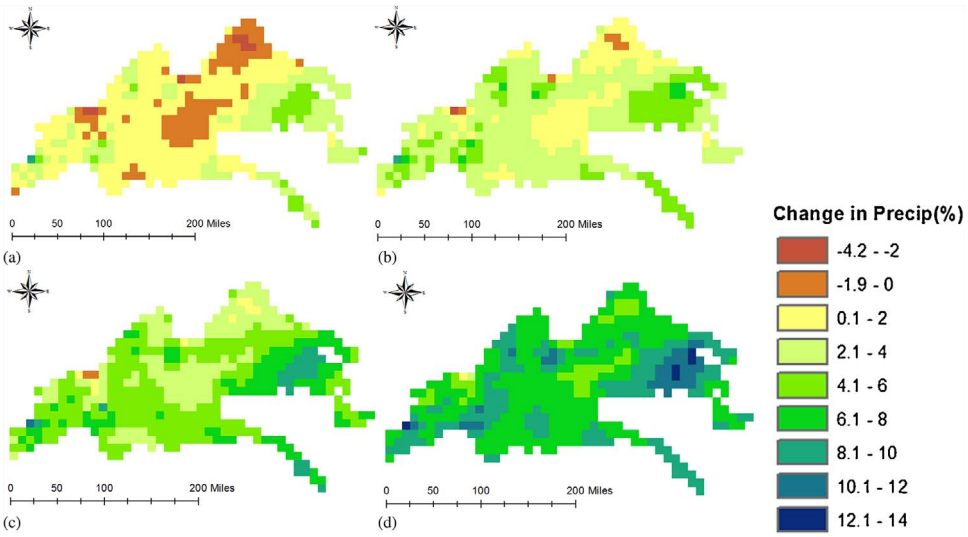

Fig. 7. Spatial maps of precipitation change for each RCP and period: (a) RCP 4.5 and f1 period (b) RCP8.5 and f1 period (c) RCP4.5 and f2 period and (d) RCP8.5 and f2 period. Negative values are represented in brown and indicate a decrease in precipitation. Positive values are represented in yellow, green, and navy, and they indicate an increase in precipitation in the future.

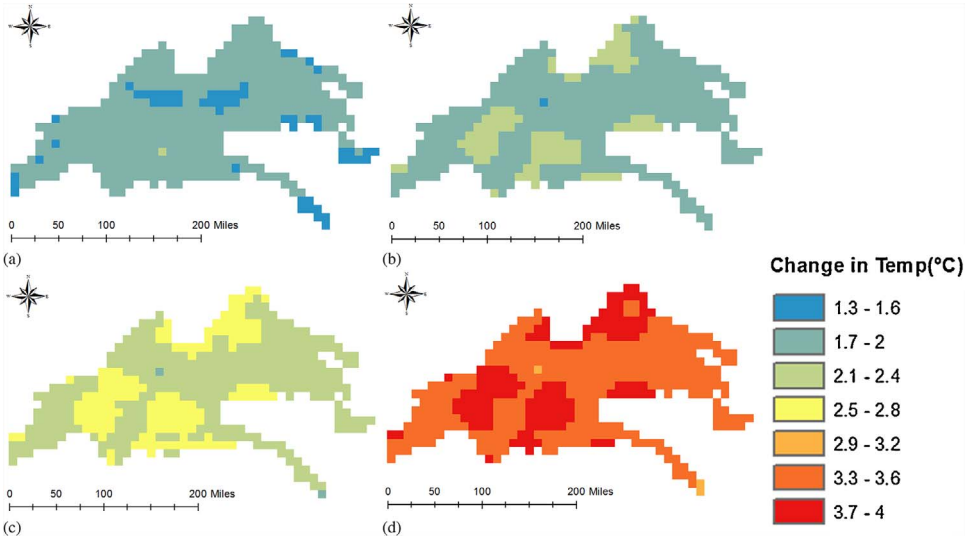

Fig. 8. Spatial maps of temperature change in each RCP and period: (a) RCP 4.5 and f1 period (b) RCP8.5 and f1 period (c) RCP4.5 and f2 period and (d) RCP8.5 and f2 period. Low increases in temperature are represented in blue, whereas high increases in temperature are represented in orange and red.

the MPDSI values accurately captured the drought conditions, which were defined by the PDSI values (−2 or less). During this period, climate division 1–6 experienced several drought events: 46, 42, 31, 25, 29, and 40 months, respectively. Fig. 10 provides a comparison of PDSI and MPDSI values. Clearly, MPDSI values based on the model results captured 62–84% of the drought conditions in this 20-year period. The highest agreement was shown in a comparison of climate division 4 and the Rappahannock River basin (84%), and the lowest agreement was shown in a comparison of climate division 5 and the James River basin (62%). There were several reasons for the low level of agreements. First, the sizes of the sub-watersheds were smaller than the climate divisions. Second, several input variables of MPDSI were not calibrated. Finally, the PET estimation methods were different for the PDSI (Thornthwaite method) and the MPDSI (Penman and Monteith method). The Thornthwaite method is based on a simple function of average surface temperature and latitude, whereas the Penman and Monteith method requires additional inputs such as wind speed, solar radiation, and water vapor content.

In this study, a parameter uncertainty analysis on drought projection was carried out, since the SWAT model is known to be highly parameterized and the parameters have the greatest influence on the model outputs (Saltelli et al., 2008). In the case of SSI, decreases in the future for both RCP 4.5 and RCP 8.5, and the f1 and f2 periods are apparent, whereas other drought indices showed increases in the mean values. The drought indices were computed using the simulated soil moisture, runoff, baseflow, and ET from the model results for both historic and future periods. The parameter uncertainty in capturing the historic index is verified with distribution and confidence intervals. The uncertainty that exists in the model-derived SSI, MSDI, and MPDSI is higher or equal for the future drought indices, and this suggests that the lower and upper bounds of future projects are somewhat similar to past conditions. It is worth mentioning that the model was calibrated for historic observations of streamflows and used for future projections. In a way, this preserved the watershed conditions that are unique to each watershed based on the results of calibration and validation from eighteen locations.

3.3. Time series of drought indices

To understand the hydrometeorological relationships between soil moisture and precipitation, a weekly assessment of the SSI, MSDI, and MPDSI were performed using SWAT-simulated water budget components. Fig. 10 shows the weekly time series of SSI for

Table 6
Ensemble means of precipitation and temperature change in the five River basins.

River basins	RCP4.5				RCP8.5			
	Change in Precipitation (%)		Change in Temperature (°C)		Change in Precipitation (%)		Change in Temperature (°C)	
	f1	f2	f1	f2	f1	f2	f1	f2
James	1.46	5.08	1.62	2.32	3.09	7.84	1.89	3.53
New	1.62	4.89	1.67	2.33	3.44	7.74	1.92	3.53
Rappahannock	0.26	3.87	1.68	2.40	1.85	7.12	1.96	3.64
Roanoke	1.12	4.93	1.71	2.38	2.88	7.66	1.96	3.56
York	2.25	5.92	1.62	2.33	3.48	8.68	1.90	3.56

Table 7
Results of calibration and validation for 18 stream gauge locations.

Station name	Type	NSE	R2	Station name	NSE	R^2
USGS02034000 (James River)	Calibration	0.59	0.59	USGS02059500 (Roanoke River)	0.60	0.62
	Validation	0.50	0.50		0.50	0.51
USGS02024000 (James River)	Calibration	0.56	0.60	USGS02062500 (Roanoke River)	0.54	0.54
	Validation	0.61	0.65		0.61	0.62
USGS02018000 (James River)	Calibration	0.48	0.48	USGS02056900 (Roanoke River)	0.46	0.50
	Validation	0.56	0.57		0.60	0.64
USGS02042500 (James River)	Calibration	0.66	0.66	USGS02077670 (Roanoke River)	0.59	0.60
	Validation	0.72	0.74		0.59	0.65
USGS02040000 (James River)	Calibration	0.63	0.64	USGS01674500 (York River)	0.65	0.67
	Validation	0.61	0.63		0.64	0.69
USGS01664000 (Rappahannock River)	Calibration	0.57	0.57	USGS01671100 (York River)	0.52	0.53
	Validation	0.49	0.52		0.50	0.52
USGS01666500 (Rappahannock River)	Calibration	0.48	0.50	USGS01673550 (York River)	0.60	0.66
	Validation	0.62	0.62		0.50	0.51
USGS03170000 (New River)	Calibration	0.41	0.55	USGS03165000 (New River)	0.62	0.63
	Validation	0.48	0.61		0.41	0.49
USGS03167000 (New River)	Calibration	0.64	0.65	USGS03161000 (New River)	0.62	0.66
	Validation	0.68	0.70		0.62	0.64

each basin and the average of all of the basins. The mean values of SSI for the historic period were 0.202 and 0.220 for RCP 4.5 and RCP 8.5. However, the mean values for the future periods were −0.117 and −0.108 for RCP 4.5, and −0.070 and −0.206 for RCP 8.5. Overall, since the results for future periods were lower than the historic means of SSI, the future droughts computed based on SSI would be presumed to increase. More specifically, the biggest difference between historic and future mean values of SSI occurred in the New River basin, and they were 0.379 in the f1 period and 0.559 in the f2 period. However, the smallest difference was seen in the Roanoke River basin for the f1 period (0.262), and the James River basin during the f2 period (0.275). The SWAT model is based on the simple water balance approach described in Eq. (1), and the increase in drought conditions based on the SSI was closely related to the input variables, such as E_a precipitation, Q_{surf}, Q_{gw}, and

Table 8 shows the differences in historic and future change of $EQ = E_a + Q_{surf} + Q_{gw}$ for both RCP 4.5 and RCP 8.5 in each river basin. EQ was calculated based on the sum of the evapotranspiration (E_a), surface runoff (Q_{surf}), and amount of return flow (Q_{gw}). As shown in Table 8, the greatest difference in EQ between historic and future periods occurred in the New River basin; they were 1.49 mm (f1) and 2.26 mm (f2) for RCP 4.5, and 1.91 mm (f1) and 3.06 mm (f2) for RCP 8.5. On the other hand, the smallest difference was seen in the James River basin during the f1 period for both RCP 4.5 (0.67 mm) and RCP 8.5 (0.84 mm), and in the Roanoke River basin during the f2 period for both RCP 4.5 (1.81 mm) and RCP 8.5 (2.32 mm). These results imply that higher differences in EQ had a great influence on drought conditions, which were estimated by SSI.

Fig. 11(a) represents the weekly time series of MSDI for the overall average of the basins. The mean values of MSDI in the historic period were −0.771 and −0.800 for RCP 4.5 and RCP 8.5. However, the mean values for the future periods were −0.478 and −0.424 for RCP 4.5, and −0.070 and −0.206 for RCP 8.5, respectively. In contrast, with the results of SSI, the mean values of MSDI for future periods were higher than the historic means of MSDI. Thus, the results imply that there was a decrease in the multivariate perspective of droughts in the future. More specifically, the biggest difference between historic and future mean values of MSDI occurred in the Roanoke River basin during the f1 period (0.355) and the James River basin during the f2 period (0.382), whereas the smallest difference occurred in the Rappahannock River during the f1 period (0.233) and the New River basin during the f2 period (0.228), respectively. Unlike the computation of SSI, MSDI was calculated using precipitation and soil moisture. Since an increase in precipitation was expected in the future periods, the evaluations of drought conditions based on MDSI were remarkably different from SSI.

Finally, Fig. 11(c) shows the weekly time series of MPDSI as the overall average of the basins. The mean values of MPDSI for the historic period were −0.110 and −0.128 for RCP 4.5 and RCP 8.5. Additionally, the mean values for future periods were 0.370 and 0.485 for RCP 4.5, and 0.398 and 0.493 for RCP 8.5, respectively. Similar to the results of MSDI, the mean values of MPDSI for future periods were larger than the historic means of MPDSI. Thus, the results imply that there was a decrease in meteorological droughts projected for the future. More specifically, the biggest difference between the historic and future mean values of MPDSI occurred in the York River basin during the f1 period (0.547), and in the Roanoke River basin during the f2 period (0.643). Whereas the smallest difference occurred in the Rappahannock River during the f1 period (0.444), and in the New River basin during the f2 period (0.57), respectively. Since MPDSI is a meteorological drought index, their values are highly influenced by increases in precipitation. Thus, the mean values of MPDSI for future periods were higher than the historic values. Additionally, the overall differences between historic and future periods of MPDSI were higher than MSDI, which can reflect both agricultural and meteorological perspectives of drought conditions.

3.4. Seasonal comparisons of drought indices

Seasonal comparisons of the historic and future drought indices are valuable to characterize what seasons are vulnerable to

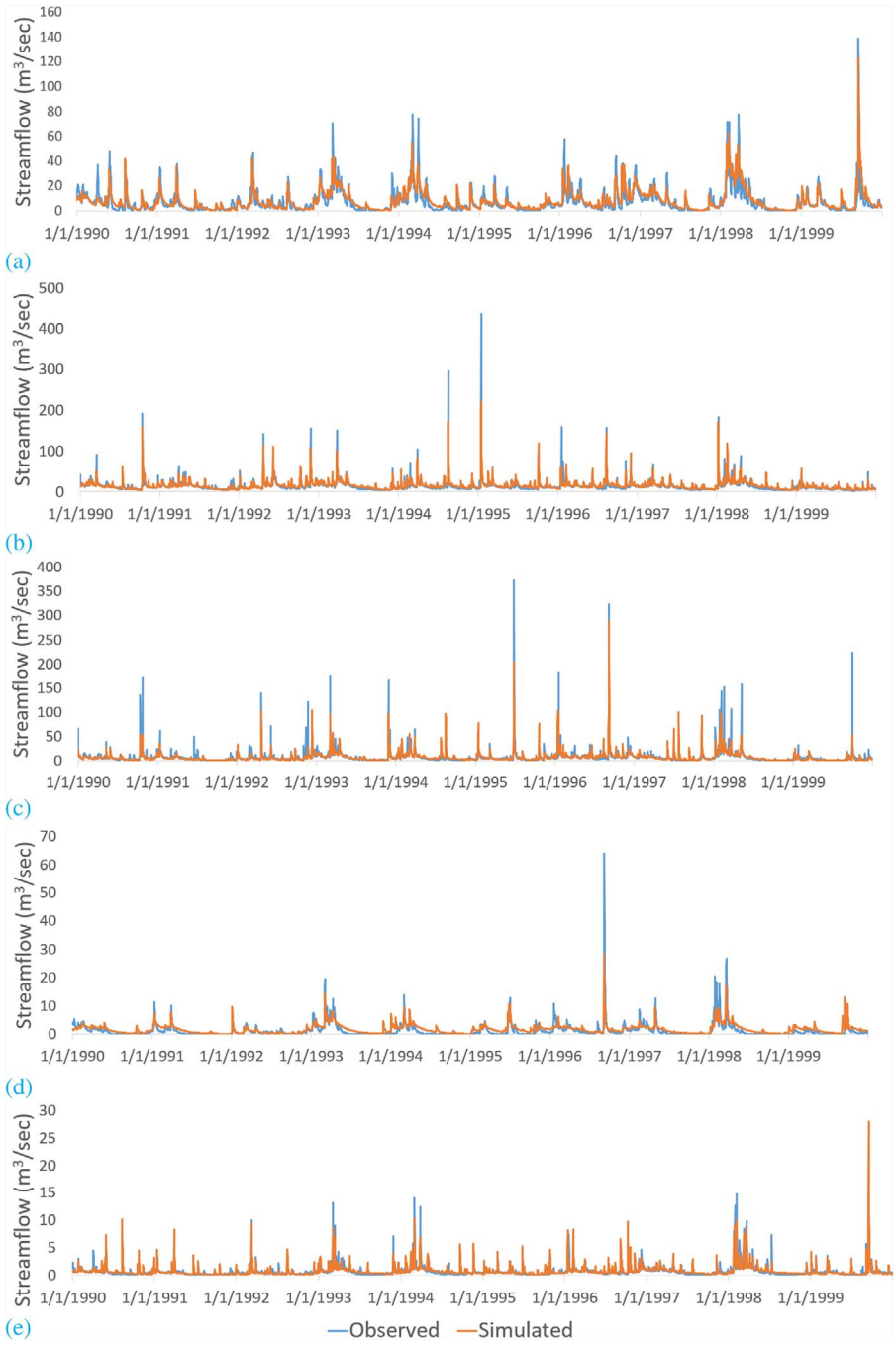

Fig. 9. The time series of observed and simulated flow from calibration at multiple locations: (a) USGS 02042500 (James River Basin) (b) USGS 0316700 (New River Basin) (c) USGS 01666500 (Rappahannock River Basin) (d) USGS 02077670 (Roanoke River Basin) (e) USGS 01673550 (York River Basin). The blue lines represent the observed flow, whereas the orange lines represent simulated flow.

drought. Thus, seasonal drought mitigation and management plans can be obtained based on these results. Specifically, evaluation of drought conditions in the crop-growing season (April to September) could have significant impacts on crop yields in Virginia (VDEM, 2013). Furthermore, drought conditions in the winter seasons are important since there is a groundwater recharge during the winter months (November to February) and it provides baseflow to streams during subsequent months.

Fig. 12 shows the seasonal comparisons of drought indices between historic and future periods in the five river basins. The results of SSI indicate that there was an overall decrease in SSI values for all weeks of the year in the future for both RCP 4.5 and RCP 8.5. Specifically, greater differences between historic and future mean values of SSI were found in the periods between April and September (approximately 13–30 weeks of year) for both the f1 and f2 periods. The results of seasonal comparisons of SSI implied that

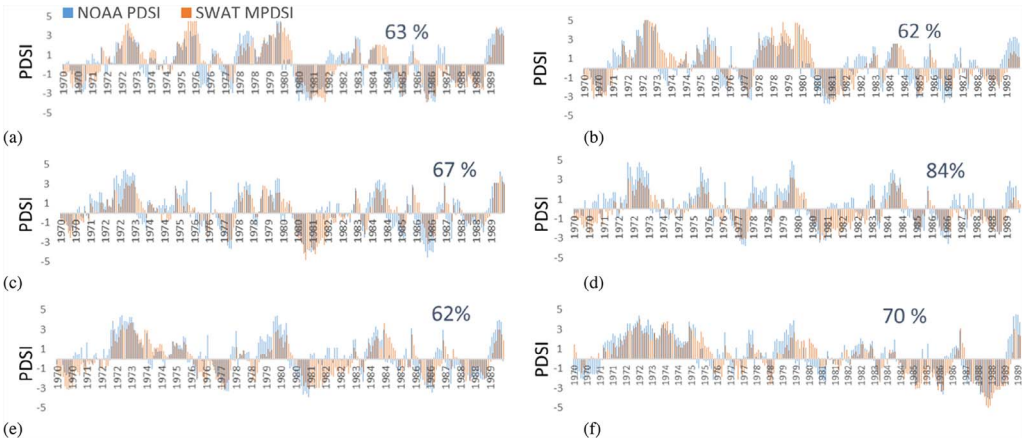

Fig. 10. Comparison of PDSI from NOAA and MPDSI from the model results. The X-axis is the 20-year period, and the Y-axis represents the drought index. (a) Climate division 1 and sub watershed no. 170 in the James river basin (b) Climate division 2 and sub watershed no. 116 in the James river basin (c) Climate division 3 and sub watershed no. 43 in the Roanoke river basin (d) Climate division 4 and sub watershed no. 15 in the Rappahannock river basin (e) Climate division 5 and sub watershed no. 64 of James river basin and (f) Climate division 6 and sub watershed no. 9 in the New river basin. The blue bars represent the PDSI values from NOAA, and the red bars represent the MPDSI values from the model results.

overall agricultural drought severities increased in the future, specifically during the crop growing seasons (April–September) in the five river basins.

In contrast, the results of MSDI show that the ensemble means of future periods were higher than the historic periods, and it implied that there was an overall decrease in drought severities from multivariate perspectives of droughts in all seasons. Similar to the time series analyses, an increase in precipitation greatly influenced the computation of MSDI, and it counterbalanced the decrease in soil moisture in the future.

However, in the New River basin for the RCP 8.5 and the f2 period, higher drought severity was expected between 15–32 weeks per year. Similar to the results of MSDI, the ensemble means of the future periods for MPDSI were higher than that of the historic means, and this indicated that there was an overall decrease in drought severities when considering variables such as precipitation, soil moisture, and evapotranspiration, which are sensitive to predicting drought.

Since climate change exhibited an increase in precipitation and temperature in the Virginia regions, future drought predictions should be conducted with reliable drought indices that can consider various hydrometeorological conditions in the future. Therefore, a drought index that can consider multiple perspectives of drought would be applicable for future drought projections.

3.5. Drought occurrences

Fig. 13 shows the spatial maps of the ratio of drought occurrences based on SSI for five river basins, and these were calculated using the division of historic and future drought occurrences for each sub-basin (future/historic). A value equal to or greater than 1 is represented in red and indicates an increase in drought occurrence in the future. However, other values less than 1 are represented in green and indicate a decrease in drought occurrences in the future. Additionally, Table 9 is the ratio of drought occurrences in future periods based on the results of SSI. As shown in Fig. 13 and Table 9, there is an overall increase in drought occurrences in the future during both f1 and f2 periods in several climate models, such as S2 and S9, for both RCP 4.5 and RCP 8.5. The results of the ensemble mean indicate that there were 1.30 times more droughts in the New River basin for RCP 8.5 during the f2 period, and 1.13–1.81 times more droughts in the Rappahannock basin. From these results, it can be said that the New and Rappahannock river basins are vulnerable to agricultural droughts among the five river basins. Additionally, the results of SSI indicate that even though there was an increase in precipitation for the simulation periods, agricultural droughts occurred more frequently in some regions. As mentioned above, the SWAT model is based on the simple water balance approach described in Eq. (1), and the increase in drought conditions was related to the input variables in E_a Eq. (1), such as precipitation, Q_{surf}, Q_{gw}, and E_a. As shown in Fig. 14, comparisons of *EQ*

Table 8
Mean values of the difference in *EQ* between historic and future periods.

River basins	RCP4.5		RCP8.5	
	f1 (mm)	f2 (mm)	f1 (mm)	f2 (mm)
James	0.67	2.05	0.84	2.58
New	1.49	2.26	1.91	3.06
Rappahannock	1.36	2.09	1.64	2.77
Roanoke	1.48	1.81	1.80	2.32
York	1.15	1.88	1.31	2.50

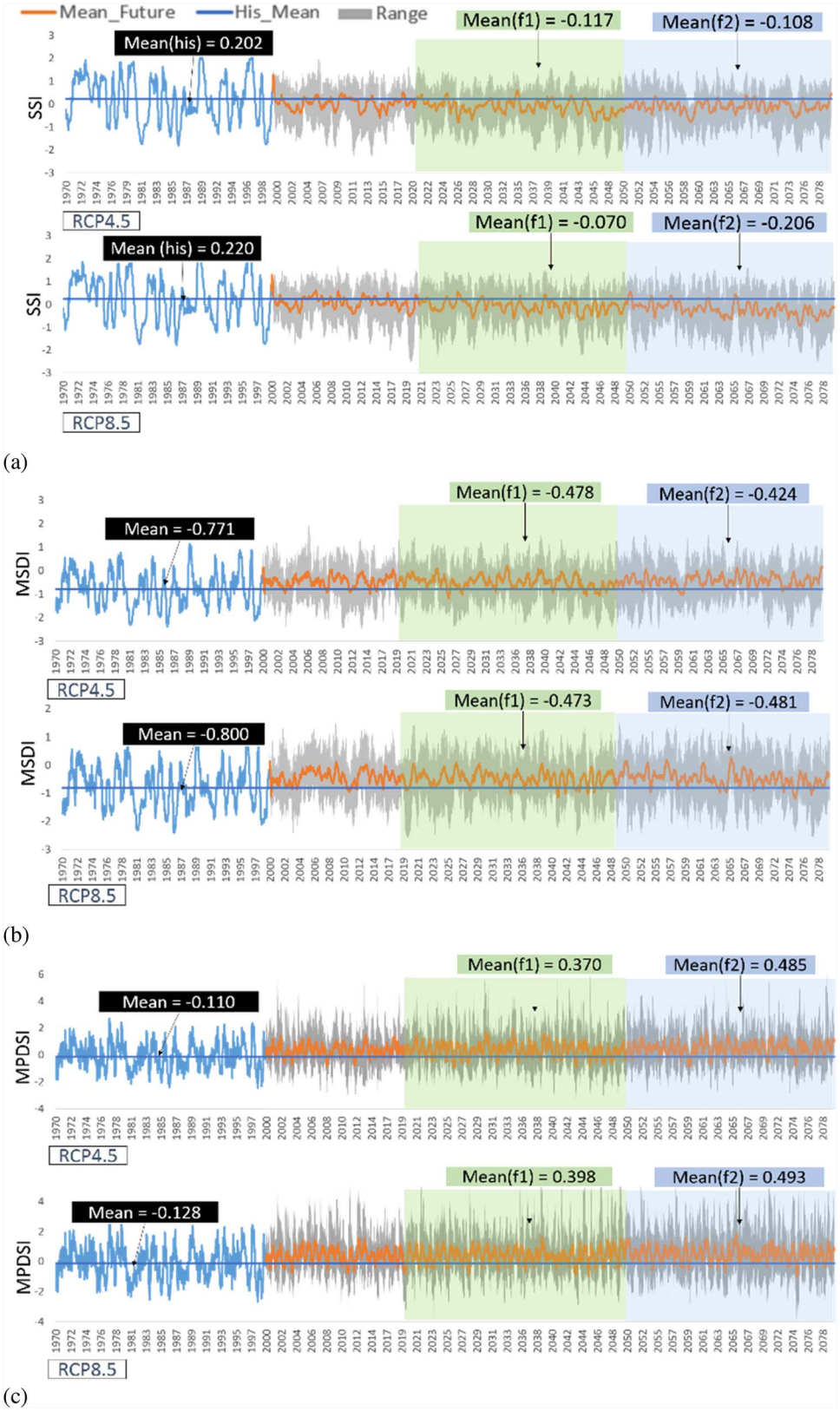

Fig. 11. Weekly time series of (a) SSI, (b) MSDI, and (c) MPDSI for each river basin. The blue lines indicate the historic period, and the orange lines are the mean values for the future period from ten climate models. The transparent green and blue rectangles highlight the future periods.

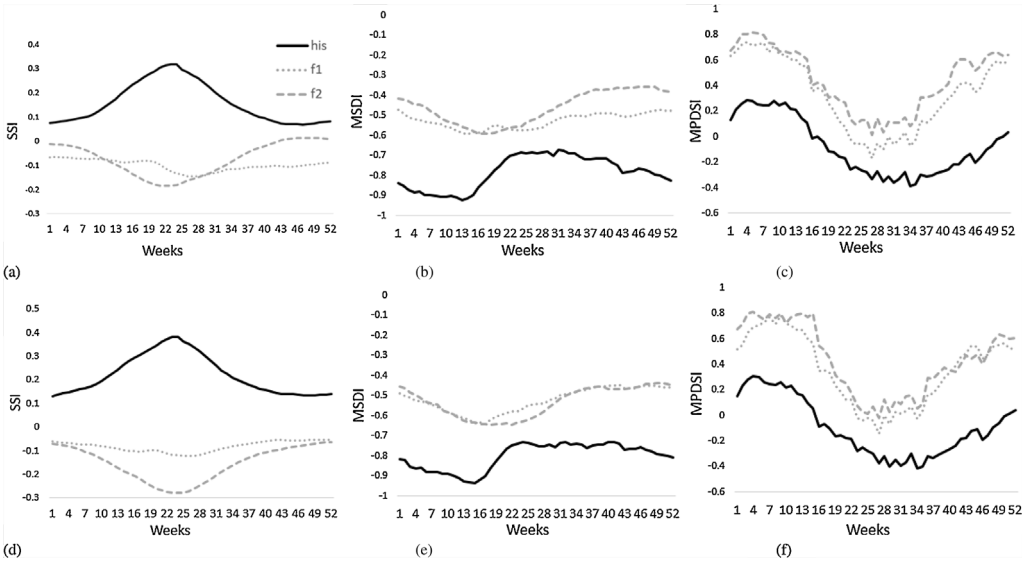

Fig. 12. Seasonal comparisons of the mean values of the drought indices in the five river basins: (a) SSI for RCP4.5 (b) MSDI for RCP4.5 (c) MPDSI for RCP4.5 (d) SSI for RCP8.5 (e) MSDI for RCP8.5 (f) MPDSI for RCP8.5.The solid lines are the weekly means of the drought indices during the historic period, whereas the dashed lines represent the future periods.

implied that increases in drought conditions based on SSI were caused by an increase in *EQ* and decrease in soil moisture.

Fig. 13 shows spatial maps of the ratio of drought occurrences based on the MSDI for five river basins, and these were calculated by dividing the historic and future drought occurrences for each sub-basin (future/historic). As shown in this figure, there was an overall decrease in drought occurrence for most of the climate models, while the areal extent also increased in S2 in the New River basin during the second future period (f2). MSDI was proposed to consider multivariate variables (precipitation and soil moisture) for drought evaluation, and it has been known that the onset and termination of droughts are influenced by both precipitation and soil moisture. Thus, drought occurrences derived by MSDI were different from SSI, which was influenced by increased precipitation in the future (Table 10).

MPDSI-based ratios in the five river basins are also shown in Fig. 13. Furthermore, Table 11 is the ratio of drought occurrences for future periods based on the results of MPDSI. There was an overall decrease in drought occurrences in the future. Since MPDSI is a meteorological drought index, it can be said that drought occurrences estimated by MPDSI are influenced by the increases in precipitation in the future (Fig. 4, Tables 5 and 6).

Fig. 14 shows the comparisons of historic and future change of $EQ = E_a + Q_{surf} + Q_{gw}$ for both RCP 4.5 and RCP 8.5 in the five river basins. The *EQ* was calculated by summing the evapotranspiration (E_a), surface runoff (Q_{surf}), and amount of return flow (Q_{gw}). As shown in Fig. 14, there was a projected overall increase in *EQ* for every week of the year in the future. Specifically, the greatest difference for RCP 8.5 and RCP 4.5 occurred during the crop-growing season. Thus, the comparisons of *EQ* implied that increases in the drought conditions based on SSI may have resulted in an increase in *EQ* and reductions in soil moisture, and, as a result, different patterns during the growing season were evident. For example, Fig. 5 shows differences in soil moisture between historic and future periods (f1 and f2) for the New river basin in the S2 model, and it indicates that increased drought based on SSI could be directly related to a soil moisture deficit.

4. Summary and conclusions

Global surface temperature has risen and is expected to continue to increase due to greenhouse gas emissions, and global climate warming would, in turn, increase regional climatic variations and their effects on droughts. Thus, reliable drought monitoring and prediction is fundamentally important to the water resource management and drought mitigation plans. Additionally, understanding various perspectives of droughts would be helpful to investigate different drought properties (e.g., meteorological and agricultural).

This study investigated future drought occurrences in the James, Roanoke, New, Rappahannock, York river basins with high-resolution analysis of future climate model datasets and multiple drought indices that were computed based on daily time step simulation results from a hydrological model (SWAT). The simulated results of runoff, evapotranspiration, and soil moisture were used to compute the drought indices. SWAT was calibrated and validated using SWAT-CUP and eighteen USGS streamflow stations, and it showed the potential for implementing the framework in other watersheds. Additionally, historical MPDSI was validated with available measured PDSI values from NOAA.

The results of the SSI-based drought occurrence analysis indicated that there was an overall increase in agricultural drought occurrences in the New River (1.3 times more) and Rappahannock (1.13–1.81 times more) River basins, and increase in drought occurrences were related to increases in ET and surface and groundwater flow. In contrast, the results of MSDI and MPDSI exhibit overall decreases in drought occurrences since both MSDI and MPDSI were affected by increases in precipitation in the future.

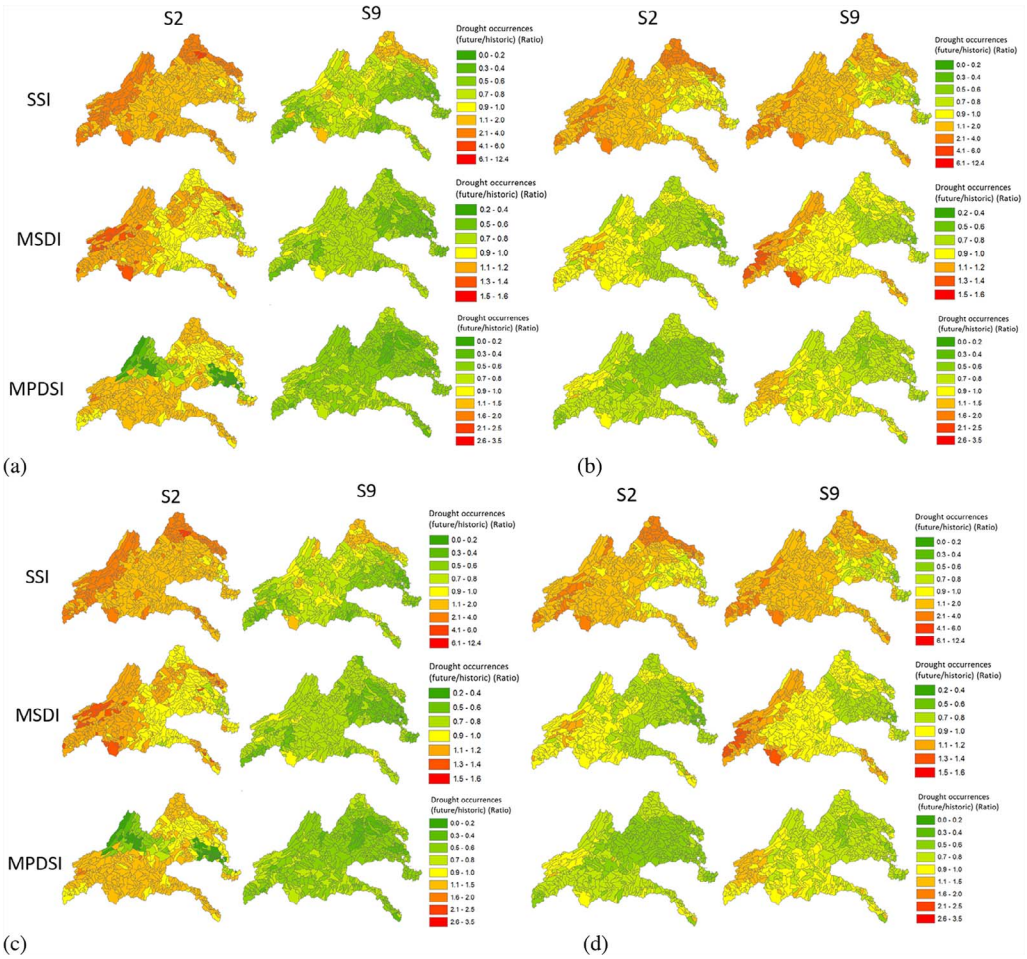

Fig. 13. Spatial maps of the comparisons of drought occurrences based on the results of SSI, MSDI, and MPDSI between the historic and the future periods: (a) RCP 4.5 and f1 period (b) RCP8.5 and f1 period (c) RCP4.5 and f2 period and (d) RCP8.5 and f2 period. A value equal to or greater than 1 is represented in red and indicates an increase in drought occurrences in the future. A value less than 1 is represented in green and indicates a decrease in drought occurrences in the future.

Therefore, potential influences from both precipitation and temperature changes should be considered in the assessment of future drought conditions.

Evaluation of future drought conditions using multiple hydrological variables derived from a hydrological model and drought

Table 9
Ratio of drought occurrences for historic and future periods in the five river basins were based on the results of SSI.

	James				New				Rappahannock				Roanoke				York			
	RCP4.5		RCP 8.5		RCP 4.5		RCP 8.5		RCP 4.5		RCP 8.5		RCP 4.5		RCP 8.5		RCP 4.5		RCP 8.5	
	f1	f2	f1	f2	f1	f2	f1	f2	f1	f2	f1	f2	f1	f2	f1	f2	f1	f2	f1	f2
S1	0.18	0.31	0.87	1.67	0.83	1.81	1.23	2.65	1.22	2.10	2.06	4.14	0.70	1.13	0.89	1.72	0.64	1.20	0.94	1.82
S2	0.61	1.62	0.80	1.17	0.76	2.26	1.03	1.89	1.40	3.13	1.54	2.50	0.63	1.65	0.79	1.33	0.67	1.50	0.75	1.12
S3	0.62	0.56	0.67	0.52	0.88	0.82	1.08	0.90	1.06	0.89	1.02	0.70	1.99	0.20	2.57	1.92	0.58	0.51	0.20	0.36
S4	0.35	0.46	0.32	0.49	0.38	0.66	0.38	0.73	0.47	0.93	0.45	0.74	0.10	0.21	0.65	1.13	0.33	0.65	0.37	0.51
S5	0.63	0.34	0.43	0.64	0.83	0.43	0.45	0.95	1.03	0.62	0.72	1.23	0.24	0.11	0.94	1.34	0.63	0.37	0.45	0.69
S6	0.39	0.52	0.66	0.81	0.51	0.73	0.89	0.95	0.54	0.85	1.26	1.35	0.39	0.58	0.63	0.80	0.35	0.57	0.66	0.82
S7	0.65	0.29	0.30	0.68	0.93	0.44	0.37	0.92	1.20	0.52	0.65	1.57	0.70	0.26	0.37	0.58	0.72	0.30	0.32	0.83
S8	0.65	0.45	0.39	0.25	0.81	0.48	0.32	0.35	1.02	0.83	0.65	0.51	0.76	0.40	0.38	0.22	0.71	0.52	0.51	0.33
S9	0.78	0.64	0.74	1.15	1.04	0.56	0.99	1.82	1.16	1.16	1.42	1.75	0.96	0.70	0.85	1.30	0.72	0.65	0.81	1.01
S10	1.04	0.90	0.82	1.47	1.28	1.24	0.88	1.86	2.20	2.34	1.92	3.63	1.10	0.87	0.94	1.42	1.08	1.13	0.89	1.67
Mean	0.59	0.61	0.60	0.89	0.83	0.94	0.76	1.30	1.13	1.34	1.17	1.81	0.76	0.61	0.90	1.18	0.64	0.74	0.59	0.92

*A value equal or greater than 1: increase in drought occurrences in the future periods.

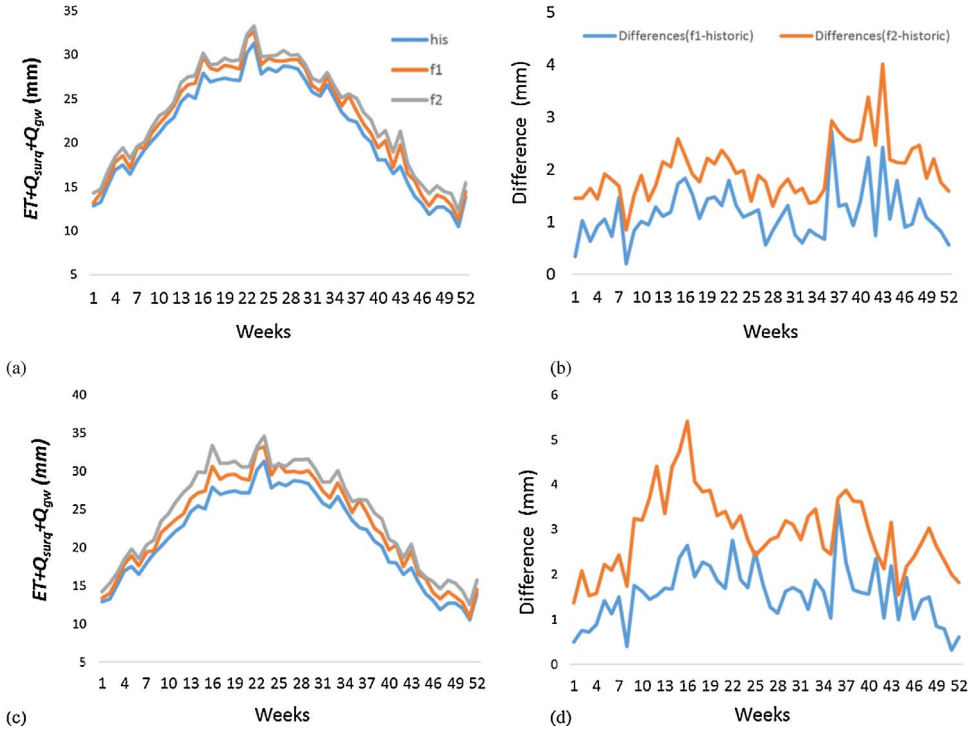

Fig. 14. Seasonal comparisons of the mean values of EQ in the five river basins. (a)RCP4.5 (c) RCP8.5 The blue lines are the weekly means of *EQ* for the historic period, whereas the orange and gray lines represent the future periods (Orange: f1, Gray: f2); (b) RCP4.5 (d) RCP8.5. Blue and orange lines are the differences in *EQ* between historic and future periods. The blue lines indicate the differences between f1 and the historic values, whereas the orange lines represent the differences between f2 and the historic values.

indices would contribute to improving drought monitoring since various factors that influence the onset, persistence of and recovery from droughts could be considered. If future drought projections were solely based on one variable such as precipitation, the river basins in Virginia would be expected to be less impacted in the future. However, even though increases in precipitation are expected in most areas of Virginia, agricultural drought occurrences in some regions are higher than in historic periods due to the increases in temperature and ET.

It is evident that identifying and determining drought occurrences is complicated, but the application of multiple drought indices at a relatively high resolution estimated by a reliable hydrological model can provide fundamental information on the evolution of future drought. Thus, the drought projection methods suggested in this study can offer insights pertinent to drought risk management and drought mitigation strategies.

Table 10
Ratio of drought occurrences for historic and future periods in the five river basins based on the results of MSDI.

	James				New				Rappahannock				Roanoke				York			
	RCP4.5		RCP 8.5		RCP 4.5		RCP 8.5		RCP 4.5		RCP 8.5		RCP 4.5		RCP 8.5		RCP 4.5		RCP 8.5	
	f1	f2	f1	f2	f1	f2	f1	f2	f1	f2	f1	f2	f1	f2	f1	f2	f1	f2	f1	f2
S1	0.51	0.54	0.66	0.85	0.68	1.04	0.86	1.12	0.69	0.82	0.74	1.01	0.68	0.79	0.72	0.89	0.57	0.72	0.62	0.81
S2	0.57	0.97	0.66	0.72	0.58	1.12	0.67	0.92	0.69	1.05	0.74	0.80	0.62	0.99	0.68	0.80	0.57	0.90	0.60	0.66
S3	0.57	0.45	0.58	0.45	0.73	0.56	0.72	0.58	0.80	0.58	0.78	0.54	0.80	0.51	0.72	0.52	0.52	0.42	0.31	0.36
S4	0.39	0.40	0.44	0.44	0.38	0.54	0.46	0.59	0.36	0.61	0.44	0.49	0.29	0.43	0.44	0.45	0.35	0.55	0.44	0.44
S5	0.60	0.34	0.41	0.56	0.70	0.42	0.43	0.72	0.67	0.39	0.48	0.68	0.46	0.26	0.44	0.54	0.57	0.34	0.42	0.54
S6	0.36	0.54	0.67	0.63	0.44	0.61	0.73	0.69	0.42	0.59	0.74	0.70	0.37	0.58	0.63	0.65	0.35	0.57	0.65	0.62
S7	0.58	0.27	0.35	0.60	0.68	0.43	0.46	0.76	0.68	0.31	0.43	0.70	0.59	0.27	0.38	0.57	0.58	0.28	0.34	0.60
S8	0.48	0.43	0.40	0.27	0.56	0.43	0.37	0.29	0.57	0.48	0.46	0.33	0.56	0.40	0.42	0.25	0.51	0.45	0.42	0.30
S9	0.71	0.60	0.71	0.83	0.94	0.65	0.79	1.12	0.70	0.66	0.79	0.84	0.87	0.69	0.80	0.92	0.65	0.57	0.71	0.77
S10	0.76	0.68	0.83	0.94	0.91	0.79	0.83	1.03	0.83	0.88	0.96	1.14	0.81	0.66	0.92	0.94	0.75	0.73	0.80	0.99
Mean	0.55	0.52	0.57	0.63	0.66	0.66	0.63	0.78	0.64	0.64	0.65	0.73	0.60	0.56	0.62	0.65	0.54	0.55	0.53	0.61

Table 11
Ratio of drought occurrences for historic and future periods in the five river basins based on the results of MPDSI.

	James				New				Rappahannock				Roanoke				York			
	RCP4.5		RCP 8.5		RCP 4.5		RCP 8.5		RCP 4.5		RCP 8.5		RCP 4.5		RCP 8.5		RCP 4.5		RCP 8.5	
	f1	f2	f1	f2	f1	f2	f1	f2	f1	f2	f1	f2	f1	f2	f1	f2	f1	f2	f1	f2
S1	0.34	0.40	0.64	0.76	0.63	0.84	0.89	0.95	0.56	0.58	0.68	0.78	0.63	0.71	0.71	0.80	0.52	0.57	0.59	0.71
S2	1.28	0.69	0.58	0.56	0.54	1.21	0.62	0.73	0.59	1.06	0.70	0.63	0.60	1.13	0.67	0.69	0.49	0.90	0.55	0.54
S3	0.58	0.44	0.56	0.47	0.74	0.49	0.74	0.49	0.95	0.65	0.82	0.65	0.73	0.70	0.75	0.59	0.53	0.42	0.22	0.20
S4	0.32	0.28	0.30	0.30	0.28	0.48	0.32	0.34	0.30	0.56	0.33	0.33	0.36	0.51	0.44	0.45	0.31	0.46	0.32	0.32
S5	0.43	0.29	0.32	0.39	0.51	0.35	0.30	0.52	0.52	0.28	0.41	0.42	0.45	0.30	0.45	0.56	0.43	0.28	0.34	0.36
S6	0.24	0.36	0.55	0.56	0.30	0.37	0.60	0.51	0.31	0.39	0.58	0.62	0.29	0.41	0.53	0.62	0.23	0.38	0.50	0.54
S7	0.39	0.17	0.24	0.43	0.52	0.35	0.37	0.57	0.47	0.21	0.34	0.49	0.47	0.21	0.28	0.45	0.38	0.15	0.24	0.40
S8	0.40	0.37	0.40	0.37	0.48	0.40	0.22	0.20	0.47	0.41	0.33	0.23	0.51	0.36	0.31	0.23	0.37	0.34	0.28	0.22
S9	0.57	0.47	0.56	0.70	0.84	0.55	0.75	1.04	0.55	0.58	0.68	0.72	0.71	0.58	0.63	0.82	0.50	0.42	0.56	0.63
S10	0.81	0.74	0.81	0.74	0.87	0.78	0.83	0.79	0.84	0.83	0.85	0.79	0.85	0.76	0.87	0.76	0.70	0.74	0.81	0.81
Mean	0.54	0.42	0.50	0.53	0.57	0.58	0.56	0.61	0.56	0.55	0.57	0.57	0.56	0.57	0.56	0.60	0.45	0.47	0.44	0.47

Acknowledgments

This work was primarily supported by the Institute for Critical Technology and Applied Science (ICTAS) at Virginia Tech. This project was funded in part by the Virginia Agricultural Experiment Station (Blacksburg) and through the Hatch Program of the National Institute of Food and Agriculture, at the United States Department of Agriculture (Washington, D.C.). We are grateful that the Advanced Research Computing facility at Virginia Tech was made available for our simulation analysis. We would like to thank the three anonymous reviewers as well as the editor for their extraordinary review and editorial comments, which helped improve the quality of the manuscript.

References

Abbaspour, K.C., 2011. SWAT-CUP4: SWAT Calibration and Uncertainty Programs–a User Manual. Swiss Federal Institute of Aquatic Science and Technology, Eawag.
AghaKouchak, A., Cheng, L., Mazdiyasni, O., Farahmand, A., 2014. Global warming and changes in risk of concurrent climate extremes: insights from the 2014 California drought. Geophys. Res. Lett. 41 (24), 8847–8852. http://dx.doi.org/10.1002/2014GL062308.
AghaKouchak, A., 2015. A multivariate approach for persistence-based drought prediction: application to the 2010–2011 East Africa drought. J. Hydrol. 526, 127–135.
Ahn, S.R., Jeong, J.H., Kim, S.J., 2015. Assessing drought threats to agricultural water supplies under climate change by combining the SWAT and MODSIM Models for the Geum River Basin, South Korea. Hydrol. Sci. J. 61 (15), 2740–2753. http://dx.doi.org/10.1080/02626667.2015.1112905.
Alley, W.M., 1984. The Palmer drought severity index: limitations and assumptions. J. Clim. Appl. Meteorol. 23 (7), 1100–1109.
Arnold, J.G., Srinivasan, R., Muttiah, R.S., Williams, J.R., 1998. Large area hydrologic modeling and assessment part I: model development1. J. Am. Soc. Water Resour. Assoc. 34 (1), 73–89.
Ashraf Vaghefi, S., Mousavi, S.J., Abbaspour, K.C., Srinivasan, R., Yang, H., 2014. Analyses of the impact of climate change on water resources components, drought and wheat yield in semiarid regions: karkheh River Basin in Iran. Hydrol. Processes 28 (4), 2018–2032.
Burke, E.J., Brown, S.J., Christidis, N., 2006. Modeling the recent evolution of global drought and projections for the twenty-first century with the Hadley Centre climate model. J. Hydrometeorol. 7 (5), 1113–1125. http://dx.doi.org/10.1175/JHM544.1.
Changnon, S.A., Pielke Jr., R.A., Changnon, D., Sylves, R.T., Pulwarty, R., 2000. Human factors explain the increased losses from weather and climate extremes. Bull. Am. Meteorol. Soc. 81 (3), 437.
Dai, A., 2011. Drought under global warming: a review. Wiley Interdiscip. Rev. Clim. Change 2 (1), 45–65. http://dx.doi.org/10.1002/wcc.81.
Dai, A., 2013. Increasing drought under global warming in observations and models. Nat. Clim. Change 3 (1), 52–58. http://dx.doi.org/10.1038/nclimate1633.
Diffenbaugh, N.S., Swain, D.L., Touma, D., 2015. Anthropogenic warming has increased drought risk in California. Proc. Natl. Acad. Sci. 112 (13), 3931–3936. http://dx.doi.org/10.1073/pnas.1422385112.
Edwards, D.C., 1997. Characteristics of 20th Century Drought in the United States at Multiple Time Scales Atmospheric Science Paper No. 634, May. pp. 1–30.
Gesch, D.B., 2007. The national elevation dataset. In: Maune, D. (Ed.), Digital Elevation Model Technologies and Applications: The DEM User's Manual, second edition. American Society for Photogrammetry and Remote Sensing, Bethesda, Maryland, pp. 99–118.
Gutzler, D.S., Robbins, T.O., 2011. Climate variability and projected change in the western United States: regional downscaling and drought statistics. Clim. Dyn. 37 (5–6), 835–849. http://dx.doi.org/10.1007/s00382-010-0838-7.
Hao, Z., AghaKouchak, A., 2013. Multivariate standardized drought index: a parametric multi-index model. Adv. Water Resour. 57, 12–18. http://dx.doi.org/10.1016/j.advwatres.2013.03.009.
Hao, Z., AghaKouchak, A., 2014. A nonparametric multivariate multi-index drought monitoring framework. J. Hydrometeorol. 15 (1), 89–101. http://dx.doi.org/10.1175/JHM-D-12-0160.1.
Homer, C., Huang, C., Yang, L., Wylie, B., Coan, M., 2004. Development of a 2001 national land-cover database for the United States. Photogramm. Eng. Remote Sens. 70 (7), 829–840. http://dx.doi.org/10.14358/PERS.70.7.829.
IPCC, 2007. Climate change 2007: the physical science basis. In: Solomon, S., Qin, D., Manning, M., Chen, Z., Marquis, M., Averyt, K.B., Tignor, M., Miller, H.L. (Eds.), Contribution of Working Group I to the Fourth Assessment Report of the Intergovernmental Panel on Climate Change. Cambridge University Press, Cambridge, United Kingdom and New York, NY, USA, pp. 996.
Jaksa, W.T., Sridhar, V., 2015. Effect of irrigation in simulating long-term evapotranspiration climatology in a human-dominated river basin system. Agric. For. Meteorol. 200, 109–118.
Jha, M., Pan, Z., Takle, E.S., Gu, R., 2004. Impacts of climate change on streamflow in the Upper Mississippi River Basin: a regional climate model perspective. J. Geophys. Res.: Atmos. 109, D9. http://dx.doi.org/10.1029/2003JD003686.
Jin, X., Sridhar, V., 2012. Impacts of climate change on hydrology and water resources in the Boise and Spokane River Basins. J. Am. Water Resour. Assoc. 1–25. http://dx.doi.org/10.1111/j.1752-1688.2011.00605.x.
Karl, T.R., Gleason, B.E., Menne, M.J., McMahon, J.R., Heim, R.R., Brewer, M.J., Kunkel, K.E., Arndt, D.S., Privette, J.L., Bates, J.J., Groisman, P.Y., 2012. US temperature and drought: recent anomalies and trends. Eos Trans. Am. Geophys. Union 93 (47), 473–474. http://dx.doi.org/10.1029/2012EO470001.

Kumar, S., Lawrence, D.M., Dirmeyer, P.A., Sheffield, J., 2014. Less reliable water availability in the 21 st century climate projections. Earth's Future 2 (3), 152–160. http://dx.doi.org/10.1002/2013EF000159.
Lakshmi, V., Piechota, T., Narayan, U., Tang, C., 2004. Soil moisture as an indicator of weather extremes. Geophys. Res. Lett. 31 (11).
Leonard, M., Westra, S., Phatak, A., Lambert, M., van den Hurk, B., McInnes, K., Risbey, J., Schuster, S., Jakob, D., Stafford-Smith, M., 2014. A compound event framework for understanding extreme impacts. Wiley Interdiscip. Rev. Clim. Change 5 (1), 113–128. http://dx.doi.org/10.1002/wcc.252.
Liu, L., Hong, Y., Looper, J., Riley, R., Yong, B., Zhang, Z., Hocker, J., Shafer, M., 2013. Climatological drought analyses and projection using SPI and PDSI: case study of the Arkansas Red River Basin. J. Hydrol. Eng. 18 (7), 809–816. http://dx.doi.org/10.1061/(ASCE)HE.1943-5584.0000619.
Loukas, A., Vasiliades, L., Tzabiras, J., 2008. Climate change effects on drought severity. Adv. Geosci. 17, 23–29. http://dx.doi.org/10.5194/adgeo-17-23-2008.
Mao, Y., Nijssen, B., Lettenmaier, D.P., 2015. Is climate change implicated in the 2013–2014 California drought? A hydrologic perspective. Geophys. Res. Lett. 42 (8), 2805–2813. http://dx.doi.org/10.1002/2015GL063456.
McKee, T.B., Doesken, N.J., Kleist, J., 1993. Drought monitoring with multiple time series. In: 8th Conference on Applied Climatology. Boston, American Meteorological Society.
Mishra, A.K., Singh, V.P., 2009. Analysis of drought severity–area-frequency curves using a general circulation model and scenario uncertainty. J. Geophys. Res.: Atmos. 114 (D6). http://dx.doi.org/10.1029/2008JD010986.
Mishra, A.K., Singh, V.P., 2010. A review of drought concepts. J. Hydrol. 391 (1), 202–216. http://dx.doi.org/10.1016/j.jhydrol.2010.07.012.
Mishra, V., Cherkauer, K.A., Shukla, S., 2010. Assessment of drought due to historic climate variability and projected future climate change in the Midwestern United States. J. Hydrometeorol. 11 (1), 46–68. http://dx.doi.org/10.1175/2009JHM1156.1.
Mishra, V., Shah, R., Thrasher, B., 2014. Soil moisture droughts under the retrospective and projected climate in India. J. Hydrometeorol. 15 (6), 2267–2292. http://dx.doi.org/10.1175/JHM-D-13-0177.1.
Mo, K.C., Chelliah, M., 2006. The modified palmer drought severity index based on the NCEP north american regional reanalysis. J. Appl. Meteorol. Climatol. 45 (10), 1362–1375. http://dx.doi.org/10.1175/JAM2402.1.
Mo, K.C., 2008. Model-based drought indices over the United States. J. Hydrometeorol. 9 (6), 1212–1230. http://dx.doi.org/10.1175/2008JHM1002.1.
Monteith, J.L., 1965. Evaporation and environment. In: Proceedings of the State and Movement of Water in Living Organisms, 19th Symposia of the Society of Experimental Biology. Cambridge University Press Swansea,UK/Cambridge, UK. pp. 205–234.
Moriasi, D.N., Arnold, J.G., Van Liew, M.W., Bingner, R.L., Harmel, R.D., Veith, T.L., 2007. Model evaluation guidelines for systematic quantification of accuracy in watershed simulations. Trans. ASABE 50 (3), 885–900. http://dx.doi.org/10.13031/2013.23153.
National Climatic Data Center (NCDC), 2002. US National Percent Area Severely to Extremely Dry and Severely to Extremely Wet.
Narasimhan, B., Srinivasan, R., 2005. Development and evaluation of soil moisture deficit index (SMDI) and evapotranspiration deficit index (ETDI) for agricultural drought monitoring. Agric. For. Meteorol. 133 (1), 69–88. http://dx.doi.org/10.1016/j.agrformet.2005.07.012.
Nash, J.E., Sutcliffe, J.V., 1970. River flow forecasting through conceptual models part I—a discussion of principles. J. Hydrol. 10 (3), 282–290. http://dx.doi.org/10.1016/0022-1694(70)90255-6.
Nasrollahi, N., AghaKouchak, A., Cheng, L., Damberg, L., Phillips, T.J., Miao, C., Hsu, K., Sorooshian, S., 2015. How well do CMIP5 climate simulations replicate historical trends and patterns of meteorological droughts? Water Resour. Res. 51 (4), 2847–2864. http://dx.doi.org/10.1002/2014WR016318.
Nelsen, R.B., 2006. An Introduction to Copulas, 2nd. ed. SpringerScience Business Media, New York, pp. 269.
Niemeyer, S., 2008. New drought indices. Water Manage. 80, 267–274. http://om.ciheam.org/article.php?IDPDF=800451.
Pachauri, R.K., Allen, M.R., Barros, V.R., Broome, J., Cramer, W., Christ, R., Church, J.A., Clarke, L., Dahe, Q., Dasgupta, P., Dubash, N.K., 2014. Climate Change 2014: Synthesis Report. Contribution of Working Groups I, II and III to the Fifth Assessment Report of the Intergovernmental Panel on Climate Change. IPCC p. 151.
Palmer, W.C., 1965. Meteorological Drought. Weather Bureau Res. Paper 45. U.S. Dept. of Commercepp. 58.
Rajsekhar, D., Singh, V.P., Mishra, A.K., 2015. Integrated drought causality, hazard, and vulnerability assessment for future socioeconomic scenarios: an information theory perspective. J. Geophys. Res.: Atmos. 120 (13), 6346–6378. http://dx.doi.org/10.1002/2014JD022670.
Reifen, C., Toumi, R., 2009. Climate projections: past performance no guarantee of future skill? Geophys. Res. Lett. 36, L13704. http://dx.doi.org/10.1029/2009GL038082.
Ross, T., Lott, N., 2003. A Climatology of 1980–2003 Extreme Weather and Climate Events. National Climatic Data Center Technical Report No. 2003–01. NOAA/NESDIS. National Climatic Data Center, Asheville, NC.
Saltelli, A., Ratto, M., Andres, T., Campolongo, F., Cariboni, J., Gatelli, D., Saisana, M., Tarantola, S., 2008. Global Sensitivity Analysis: the Primer. John Wiley & Sons.
Schuol, J., Abbaspour, K.C., Yang, H., Srinivasan, R., Zehnder, A.J.B., 2008. Modeling blue and green water availability in africa. Water Resour. Res. 44 (7), W07406. http://dx.doi.org/10.1029/2007WR006609.
Sehgal, V., Sridhar, V., Tyagi, A., 2017. Stratified drought analysis using a stochastic ensemble of simulated and in- situ soil moisture observations. J. Hydrol. 545, 226–250. http://dx.doi.org/10.1016/j.jhydrol.2016.12.033.
Sheffield, J., Wood, E.F., 2008. Projected changes in drought occurrence under future global warming from multi-model, multi-scenario, IPCC AR4 simulations. Clim. Dyn. 31 (1), 79–105. http://dx.doi.org/10.1007/s00382-007-0340-z.
Sheffield, J., Wood, E.F., Roderick, M.L., 2012. Little change in global drought over the past 60 years. Nature 491, 435–440. http://dx.doi.org/10.1038/ nature11575.
Sridhar, V., Anderson, K.A., 2017. Human-induced modifications to boundary layer fluxes and their water management implications in a changing climate. Agric. For. Meteorol. 234, 66–79. http://dx.doi.org/10.1016/j.agrformet.2016.12.009.
Sternberg, T., 2011. Regional drought has a global impact. Nature 472 (7342), 169. http://dx.doi.org/10.1038/472169d.
Strzepek, K., Yohe, G., Neumann, J., Boehlert, B., 2010. Characterizing changes in drought risk for the United States from climate change. Environ. Res. Lett. 5 (4), 044012.
Swain, D.L., Tsiang, M., Haugen, M., Singh, D., Charland, A., Rajaratnam, B., Diffenbaugh, N.S., 2014. The extraordinary California drought of 2013/2014: character, context, and the role of climate change. Bull. Am. Meteorol. Soc. 95 (9), S3.
Tallaksen, L.M., Van Lanen, H.A., 2004. Hydrological Drought: Processes and Estimation Methods for Streamflow and Groundwater Vol. 48 Elsevier.
Thornthwaite, C.W., 1948. An approach toward a rational classification of climate. Geogr. Rev. 38 (1), 55–94.
Tsakiris, G., Loukas, A., Pangalou, D., Vangelis, H., Tigkas, D., Rossi, G., A, et al., 2007. Cancelliere. Drought Characterization. Drought Management Guidelines Technical Annex 85–102.
USDA Soil Conservation Service (USDA), 1972. National Engineering Handbook, Hydrology, Section 4, Chapters 4–10. GPO, Washington, DC.
U.S. Department of Agriculture (USDA), 1991. State Soil Geo-graphic (STATSGO) Database: Data Use Information. Miscella-neous Publication Number 1492. Washington, D.C.
Virginia Department of Emergency (VDEM), 2013. Commonwealth of Virginia Hazard Mitigation Plan. Chapter 3: Hazard Identification and Risk Assessment.
Vasiliades, L., Loukas, A., 2009. Hydrological response to meteorological drought using the Palmer drought indices in Thessaly, Greece. Desalination 237 (1), 3–21.
Wang, D., Hejazi, M., Cai, X., Valocchi, A.J., 2011. Climate change impact on meteorological, agricultural, and hydrological drought in central Illinois. Water Resour. Res. 47 (9), W09527. http://dx.doi.org/10.1029/2010WR009845.
Wang, J., Kessner, A.L., Aegerter, C., Sharma, A., Judd, L., Wardlow, B., You, J., Shulski, M., Irmak, S., Kilic, A., Zeng, J., 2016. A multi-sensor view of the 2012 central plains drought from space. Front. Environ. Sci. 4, 45. http://dx.doi.org/10.3389/fenvs.2016.00045.
Wang, G.L., 2005. Agricultural drought in a future climate: results from 15 global climate models participating in the IPCC 4th assessment. Clim. Dyn. 25 (7–8), 739–753.
Wilhite, D.A., Hayes, M.J., 1998. Drought planning in the United States: status and future directions. The Arid Frontier. Springer, Netherlands, pp. 33–54.
Wu, K., Johnston, C.A., 2007. Hydrologic response to climatic variability in a Great Lakes Watershed: a case study with the SWAT model. J. Hydrol. 337 (1), 187–199. http://dx.doi.org/10.1016/j.jhydrol.2007.01.030.
Wuebbles, D.J., Kunkel, K., Wehner, M., Zobel, Z., 2014. Severe weather in United States under a changing climate. Eos Trans. Am. Geophys. Union 95 (18), 149–150. http://dx.doi.org/10.1002/2014EO180001.
Zargar, A., Sadiq, R., Naser, B., Khan, F.I., 2011. A review of drought indices. Environ. Rev. 19, 333–349.